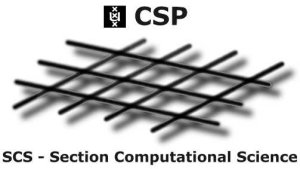

Microsimulation of Financial Markets

MSc Thesis (*Afstudeerscriptie*)

written by

Wang, Zhengdao

under the supervision of **Dr. Drona Kandhai**, **Drs. Guangzhong Qiu** and **Prof. Peter Sloot**, and submitted to the Board of Examiners in partial fulfillment of the requirements for the degree of

MSc in Computer Science

at the *Universiteit van Amsterdam.*

November, 2005

Faculteit der Natuurwetenschappen, Wiskunde en Informatica

Abstract

The complex dynamics of financial markets can be characterized by some stylized facts of which the most important ones are: non-Gaussian distribution of return, short-term autocorrelation of return and long-term autocorrelation of volatility. Up to now, the traditional economic and financial theories cannot explain these satisfactorily. As complementary approach to the traditional ones, microsimulation have shown its strengths in studying the complex dynamics in economic and financial systems. In this thesis, we first describe the stylized facts by means of empirical data analysis. After a general discussion of the microsimulation methodology, we study three well-known microsimulation models out of the many that have been developed so far: the Cont-Bouchaud model, the Lux-Marchesi model and the model by Bak et al. We have performed numerical experiments with these models for a wide range of parameters. These numerical studies elaborated that all three models can generate non-Gaussian distribution of return, but only two of them (the Lux-Marchesi model and the model by Bak et al) can confirm the volatility clustering phenomenon. In addition, from these case studies, we have obtained some insights with respect to the common mechanisms that account for these two stylized facts. Based on this, we have proposed two alternative ways to improve the Cont-Bouchaud model. It is demonstrated that both proposed methodologies can generate volatility clustering. In general, our results suggests that the non-Gaussian distribution of return is caused by the herding behavior of agents, while volatility clustering is connected with the change in activity level which might be caused by different economic factors. Finally some recommendations are given for future research.

Contents

List of Figures

List of Tables

Chapter 1

Introduction

1.1 Background

The dynamics of financial markets is highly complex. Up to now, the main stream financial theories still lack a satisfactory explanation of its origin. The complexity of the dynamics can be characterized by some stylized facts, e.g., non-Gaussian (fat-tailed) distribution of return[1], relatively fast decay of the autocorrelation of return, and long term autocorrelation of volatility[2].

Traditional analysis of the financial time series (based on statistical techniques) fails to give a definite answer for the presence of these stylized facts [28]. This is interesting but not surprising. Financial markets are composed of many heterogeneous traders and different types of financial assets. The complexity of the dynamics of financial markets is not only because of their great number of elements, their complex structure with respect to how the elements are located and linked to each other, but also due to the collective behavior of the interacting elements under the influence of massive external factors. Without considering the highly non-linear interaction at this microscopic level, it is hard to describe properly the aggregative dynamics of financial markets. Thus, at least as a complementary approach in economics and finance, we should deal with the dynamics at the micro level.

Recently, the technique of microsimulation, which has been successfully applied in natural sciences, has been used by researchers in economics and finance. With this technique, we start with modeling the market, the behavior of agents and the interactions between them. Then we can simulate the dynamics of interest and study the complexity of the dynamics from bottom up. Many microsimulation models have been developed in the recent years. The technique

[1] The basic definition of return is $R(t+1) = [P(t+1) - P(t)]/P(t)$, where $R(t)$ is return at time t, $P(t)$ is price at time t and so on. When continuous compounding is taken into account, it becomes $R(t+1) = ln(P(t+1)) - ln(P(t))$, which is more widely used in financial analysis. More detailed discussion about the definition of return will be presented later in this thesis.

[2] Volatility is defined as the standard deviation of a sample of returns over a period of time T. By setting $T = 1$ we have the absolute value of return over one unit time period $|r|$, which is the most commonly used proxy for volatility in practice. The other commonly used form of volatility is the square of return, r^2. There is a more detailed discussion about the definition of volatility later in this thesis.

has already shown its advantages. Many microscopic models are able to confirm (some of) the main stylized facts.

However, as we will demonstrate in this thesis, there are still some problems in this field. For instance, even some well-known models, e.g., the Cont-Bouchaud model [6], can not generate some important stylized facts. Moreover, although many models can generate the main stylized facts, they differ from each other in fundamental aspects in how to model the market and its dynamics. This implies that a common realization of the mechanisms that accounts for the complex dynamics of financial markets has not yet been achieved in this field [13].

1.2 Motivation

The problems in this field, as discussed above, motivate us to perform a detailed study of three well-known microsimulation models by the following approaches:

1. Implementation: We will implement the microsimulation models and perform numerical experiments in order to thoroughly understand their modeling principles.

2. Parameter study: We will perform parameter study and compare the relevant characteristics of the simulation results with the stylized features known from empirical data, in order to identify advantages and shortcomings (if any) of the models. Especially, we will investigate the reasons why they do confirm or fail to confirm the stylized facts.

3. Improvement: We will improve (if possible) the models such that they can overcome the shortcomings.

4. General understanding of the origins of the stylized facts: We will try to identify the common grounds for the various models in terms of a fundamental mechanism that explains the complex dynamics.

We believe that being able to generate the stylized facts is a prerequisite for a good microsimulation model. However, we also think that this alone is not enough. As T. Lux [18] has pointed out, even though those models reproduce the essential stylized facts as observed in real financial time series, a deeper understanding of the underlying processes still remains difficult. The general objective of this master thesis project is to contribute to the further understanding of the complex dynamics of financial markets through microsimulation.

1.3 Outline

The reminder of this thesis is organized in five additional chapters. Chapter 2 discusses the main stylized facts as observed in empirical financial time series. Chapter 3 gives a brief introduction to microsimulation and its applications in finance. Chapter 4 describes three well-known microsimulation models including our simulation results. Chapter 5 further analyzes the drawback of the

Cont-Bouchaud model, and presents our work on its improvement. In Chapter 6, we conclude this research and provide our ideas for future research on this topic.

Chapter 2

Stylized Facts Observed in Financial Markets

For the last decades, some theories, techniques and tools from different disciplines, e.g. economics, mathematics, physics and computer science, etc., have been applied to investigate and analyze the dynamics of financial markets. Especially, thanks to the advanced computational technology, massive amounts of high frequency financial data obtained at different frequencies became available and highly accessible. The analysis of these financial time series greatly contributed to a better understanding of the complex dynamics.
Obviously, a thorough study of empirical financial data is a good starting point of the modeling of financial markets. For this sake, in this chapter, we will give a brief description of the data available in financial markets and, in particular, we will discuss main stylized features observed in the financial time series.

2.1 Financial Data

Modern financial markets generate a huge amount of data — tens of thousands of transactions are recorded in a second. Furthermore, most of the data sets are recorded on different time scales and in different formats. Historical financial data have been recorded on different sampling rates [20] :

1. daily basis, since the middle of 19th century;
2. one minute or less, since 1984;
3. tick-by-tick (the sampling time correspond to the time of the actual transaction), since 1993.

Apart from sampling rate, the different data sets are obtained in different time windows. The time windows are typically based on the trading time of the corresponding financial market. For example, the typical open hours of stock markets are from 9.00 am to 17.00 pm. An extreme case is the market of foreign exchange, which is open for 24 hours. In a financial data set there is usually information on opening price, closing price, maximum and minimal price, and price during a day.

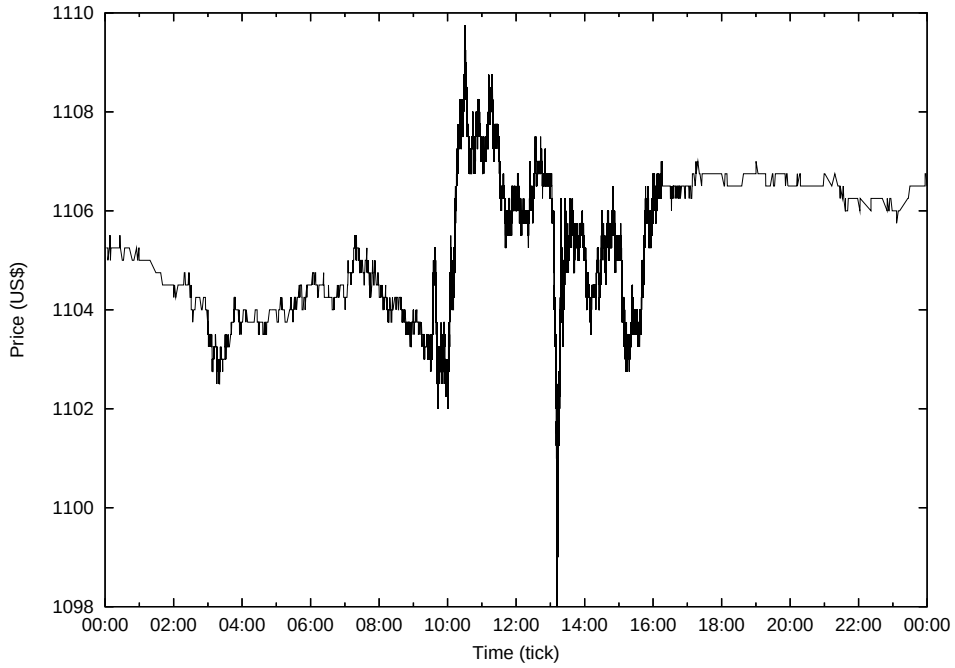

Figure 2.1: Time evolution of the S&P 500 index, from 00:00:01 am to 23:59:59 am on the September 1st, 2004. The data are sampled on a tick-by-tick basis.

2.1.1 Price and Price Changes

We start our work with analyzing the Standard & Poor's 500 (S&P 500) index [1] historical data[2]. We study two data sets based on different time scales. One contains high frequency tick-by-tick data during one day on September 1st, 2004, with frequency less than one transaction per 30 seconds. The other contains daily records for the 35 years period from 1970 to 2005. Figure 2.1 and Figure 2.2 display the price trajectories based on these two data sets.

There are different ways for describing price changes in financial time series. The most straightforward choice is to use the price change itself:

$$\Delta P(t) = P(t + \Delta t) - P(t). \tag{2.1}$$

One problem of this definition is that it does not take into account the

[1] " A stock market index is a listing of stocks, statistically reflecting the composite value of its components. It is used as a tool to represent the characteristics of its component stocks, all of which bear some commonality such as trading on the same stock market exchange, belonging to the same industry, or having similar market capitalizations. Many indexes compiled by firms of news or financial services are used to benchmark the performance of portfolios such as mutual funds."[27].

[2] "The Standard & Poor's 500 index (S&P 500) is usually considered the benchmark for U.S. equity performance. As the name suggests, the S&P 500 consists of 500 companies from a diverse range of industries and represents approximately 70% of the value of the U.S. equity market. The listed companies are highly diverse, spanning every relevant portion of the U.S. economy. Investigation on such classical index data will give us a good start for our research step to financial market."[1].

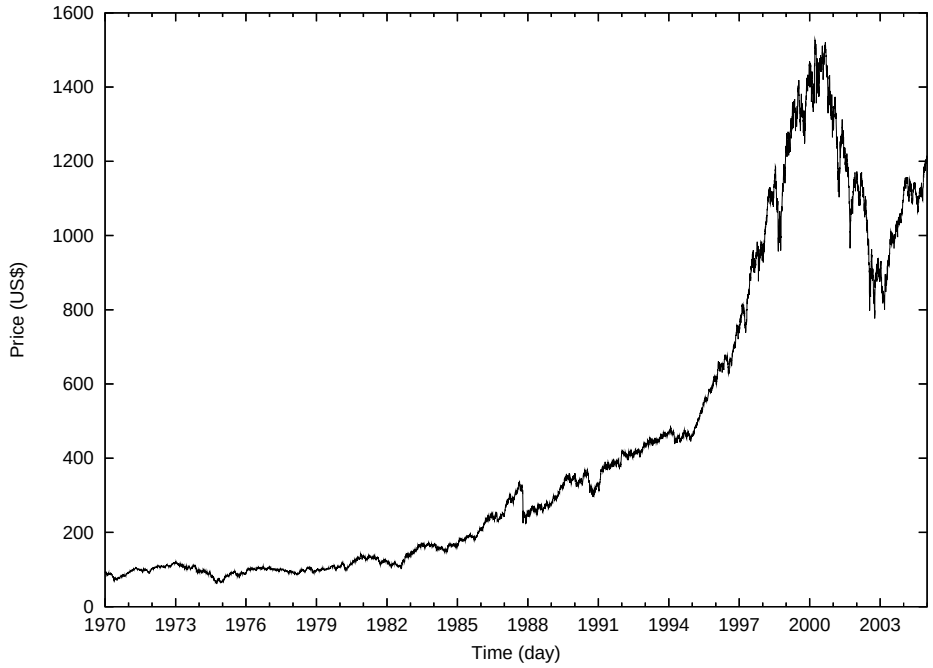

Figure 2.2: Time evolution of the price of the S&P 500 index from December 1964 to September 2005. The data are sampled on a daily basis.

change in the price due to inflation or interest payments. A more precise definition is to include a correction term in the definition,

$$Z(t) = [P(t + \Delta t) - P(t)]D(t). \tag{2.2}$$

where $D(t)$ can be a deflation factor, or a discounting factor. The merits of this approach are that (i) nonlinear transformation is not needed and (ii) prices are given in terms of 'constant' money-gains possible with risk-less investments accounted for by the factor $D(t)$. The problems are that deflator and discounting factors are unpredictable over the long term, and there is no unique choice for $D(t)$ [20]. For the present work we will focus on high frequency data that span a short time scale (day or shorter) and therefore these effects can be ignored.

Another problem of this description is that it defines price change in an absolute sense, while it is more appropriate to use a relative norm. A much more widely used measure of price change (*i.e.* profitability), which is free of this problem, is *return*.

2.1.2 Return

In finance, the term *return on investment*, or simply *return*, is used to refer to the measurement of the change in an asset's or a portfolio's accumulated value over a period of time. Usually denoted by $R(t)$ or $r(t)$, return can be described by the following quantities:

- gross return
$$R(t) = \frac{P(t+\Delta t)}{P(t)}. \tag{2.3}$$
- net return
$$R(t) = \frac{P(t+\Delta t) - P(t)}{P(t)}. \tag{2.4}$$
- log-return
$$R(t) = lnP(t+\Delta t) - lnP(t). \tag{2.5}$$

The merit of the first two definitions is that they provide a direct percentage of gain or loss in a given time period. The problem of them is their sensitivity to scale changes for long time horizons. Notice that Equation (2.4) can also be written as:
$$P(t+\Delta t) = P(t)(1+R(t)). \tag{2.6}$$
Suppose that *compounding frequency*[3] is m times per year. Then this equation can be written as:
$$P(t+\Delta t) = P(t)(1+R(t)/m)^m. \tag{2.7}$$
With *continuous compounding*[4], the equation can be approximate as:
$$P(t+\Delta t) = P(t)e^{R(t)}, \tag{2.8}$$

from which we get Equation (2.5), the definition of log-return. Being relative and dimensionless, it can be directly used to compare assets with different prices.

For high-frequency data, and data that are recorded in short time periods and influenced very weakly by inflation, all the commonly used measures listed above are approximately equivalent. However, for investigations over a long time period, log-return is used more often. Figure 2.3 shows the evolution of time series of log-return of the S&P 500 daily data. We see some very large spikes and bulks of related large returns. These phenomena will be discussed in more detail in the next section.

2.2 Stylized Facts of Financial Time Series

There are some nontrivial statistical properties in the financial time series of different markets, types of assets and time periods. These common features are called *stylized facts* [8].

In this section, by taking some empirical financial time series as examples, we will introduce the main stylized facts, namely: Non-Gaussian distribution of returns, short term correlation of return, and long term autocorrelation of volatility related to volatility clustering.

[3]Compounding is the process of accumulating the time value of money forward in time. The number of compounding periods in a year is called compounding frequency.

[4]A compounding process when m tends to infinity.

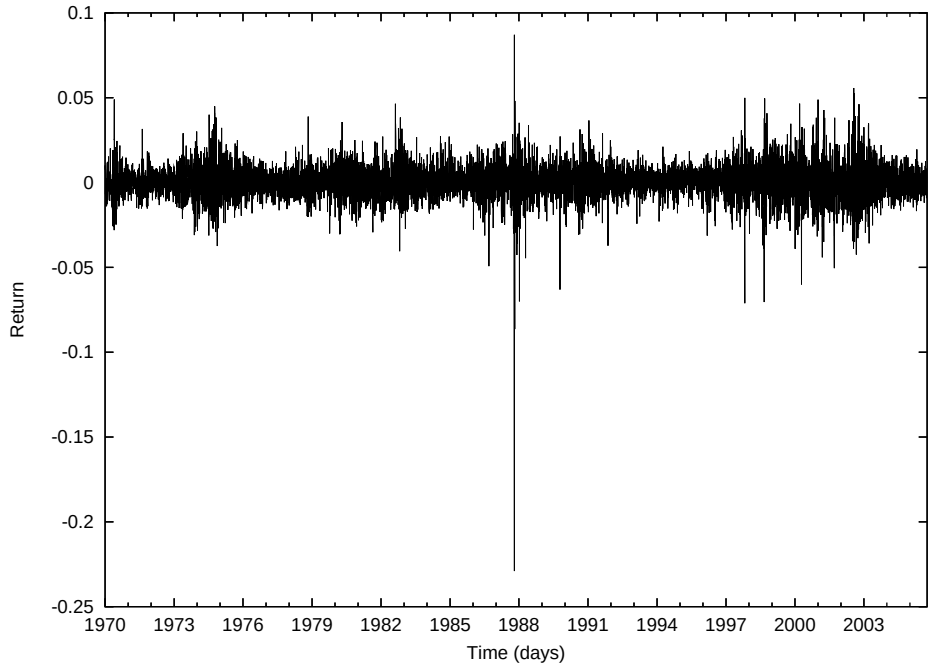

Figure 2.3: Time series of S&P 500 daily log-return from January 1970 to September 2005.

2.2.1 Non-Gaussian Distribution of Return

The statistical study of return of financial assets can be traced back to the early years of the 20th century, in which financial return was regarded as a random process [4]. Even until now, some notable economic models are based on the assumption that relative changes of price follow a Gaussian distribution. One example is the *Black-Scholes* model for option pricing. In 1963, Mandelbrot [19] pointed out that a normal distribution for modeling the asset returns is not valid in general. This is due to the heavy-tailed character of the distribution of financial returns. For this reason he suggested that financial returns should be described by the Lévy stable distribution [9]. Since then, the non-Gaussian character of distributions of financial return has been studied intensively. In Figure 2.4, we display the time series of S&P 500's daily return together with the time series of a variable that follows a Gaussian distribution. Compared to the Gaussian time series, the empirical financial time series exhibit some very large changes and clusters of large variability. For example, there is a large stroke around the end of 1987 which denotes the crash on the *Black Monday*, October 19, 1987, when the S&P 500 Index lost 20.5%! There are also some turmoils around the end of 2001, when a 15% price drop occurred within a few weeks after September 11, 2001.

The probability density function (PDF) of return is characterized by a higher and narrower peak and heavier tails compared to a Gaussian distribution. Figure 2.5 presents the histogram of the daily returns of S&P 500 from January 1970 to September 2005. Noticed that we are using a logarithmic scale for the

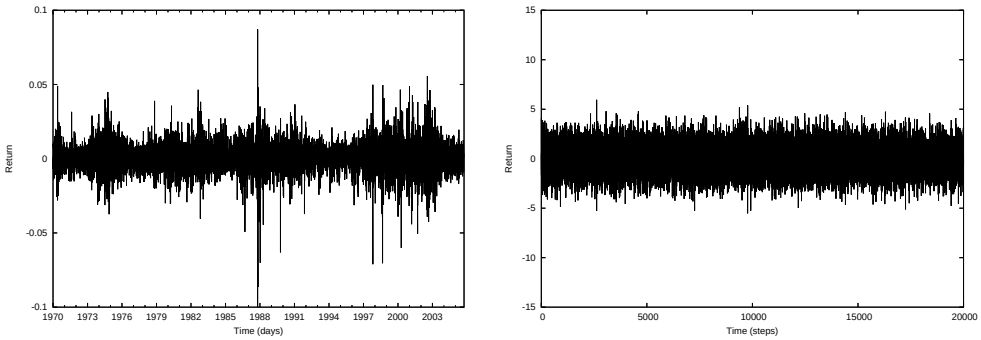

(a) Time series of return of S&P 500.

(b) Time series of a Gaussian variable.

Figure 2.4: Comparison between the return of S&P 500 and a Gaussian process.

y axis. Similar result can also be found in Figure 2.6, which shows histogram of returns of S&P500 on tick scale.

One way to measure the normality of a distribution is its *Kurtosis*, κ, which is defined as:

$$\kappa = \frac{\mu_4}{\sigma^4}. \tag{2.9}$$

where μ_4 is the fourth central moment and σ is the standard deviation of the distribution.

A data set with a high kurtosis value will have a distinct peak near the mean, declines rather rapidly around the mean, and then decays slowly leading to heavy tails. The kurtosis of a normal distribution is 3. Kurtosis less than 3 indicates a distribution that is flat at the mean and decays fast, while kurtosis larger than 3 indicates a distribution with a sharp peak and heavy tails.

In Table 2.2.1, the kurtosises of the log-returns of S&P 500 and DJIA[5] of different time series are presented. The kurtosis of S&P 500 tick-by-tick data and daily data are 26.96 and 5.95, respectively, consistent with the return distributions shown in Figure 2.6 and Figure 2.5. It can be noticed that tick and daily data usually give rise to kurtosis values larger than 3, implying that the tails of the corresponding distribution of return decay much slower than that of a normal distribution. Especially, the kurtosis of the returns of tick data is much greater than that of daily returns, deviating more from the Gaussian distribution.

[5]Dow Jones Industrial Average. It is comprised of 30 of the largest companies in the United States over a range of industries except for transport and utilities. The major difference between it and S&P 500 is that the DJIA includes a price-weighted average of 30 stocks whereas the S&P 500 is a market value-weighted index of 500 stocks.

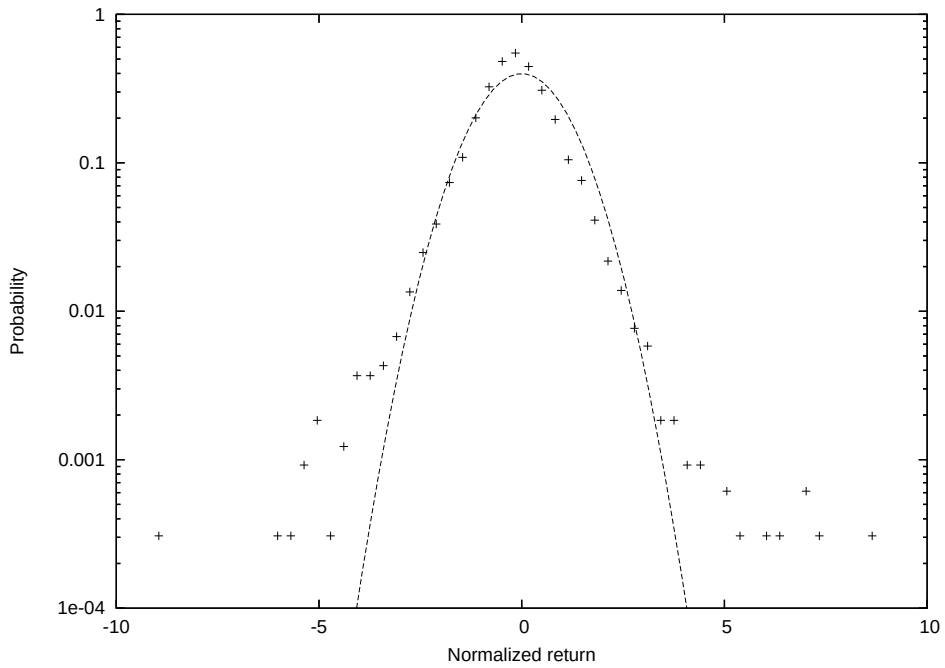

Figure 2.5: PDF of daily return of S&P 500 from January 1970 to September 2005 (the crosses) together with a Gaussian PDF (dotted line) for comparison.

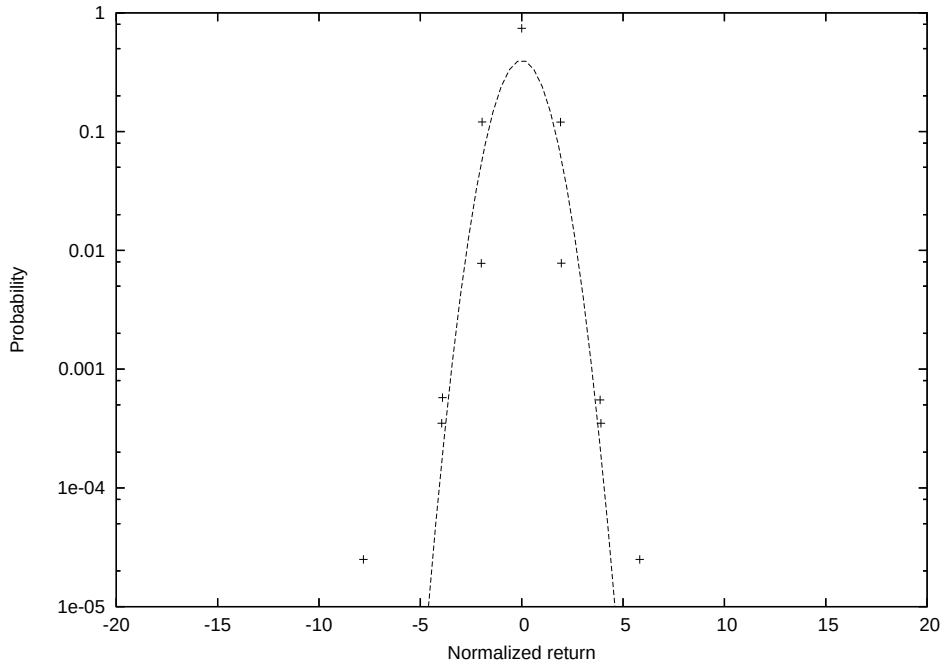

Figure 2.6: PDF of return on tick scale of S&P 500 data on September 1st, 2004 (the crosses), together with a Gaussian PDF (dotted line) for comparison.

Table 2.1: Kurtosises of empirical time series of return.

Data	*Kurtosis*
S&P 500 tick data	26.96
S&P 500 daily data	5.95
DJIA tick data	20.1056
DJIA daily data	5.7348

2.2.2 Short-term Autocorrelation of Return

Traditionally, people thought that the prices or returns in liquid markets do not have time dependence. It has been taken as a strong support to the "efficient market hypothesis (EMH)[6]". It is easy to understand that if there are correlations among price changes, there will be certain *statistical arbitrage opportunities* [7] that attract arbitrageurs. Those statistical arbitrage will eventually eliminate the correlations, except on very small time scales that represents the amount of time the market takes to react on the arrived information.

Temporal independence of returns can be quantified by analyzing its autocorrelation function (ACF):

$$c(\tau) = \frac{\sum_{t=1}^{N-\tau}(Y_t - \bar{Y})(Y_{t+\tau} - \bar{Y})}{\sum_{t=1}^{N}(Y_t - \bar{Y})^2}. \tag{2.10}$$

where N denotes the total number of time steps, Y_t the return at time t, and $\bar{Y}$ the mean of the returns.

The results of the autocorrelation function of the S&P 500 daily return and tick return are shown in Figure 2.7 and Figure 2.8, respectively. For comparison, in these figures and all plots that follow, we include corresponding results obtained for a series of independent normal distributed variables.

The results indicate that the autocorrelation of daily returns quickly drops to the noise range. However, obvious autocorrelations can be observed in the tick returns for the time lag from 0 to 25 ticks (about a few minutes). This suggests that financial returns have very short time 'memory'.

[6] "An 'efficient' market is defined as a market where there are large numbers of rational, profit-maximizers actively competing, with each trying to predict future market values of individual securities, and where important current information is almost freely available to all participants. In an efficient market, competition among the many intelligent participants leads to a situation where, at any point in time, actual prices of individual securities already reflect the effects of information based both on events that have already occurred and on events which, as of now, the market expects to take place in the future. In other words, in an efficient market at any point in time the actual price of a security will be a good estimate of its intrinsic value." [11].

[7] "An attempt to profit from pricing inefficiencies that are identified through the use of mathematical models. Statistical arbitrage attempts to profit from the likelihood that prices will trend toward a historical norm. Unlike pure arbitrage, statistical arbitrage is not risk-less." [2].

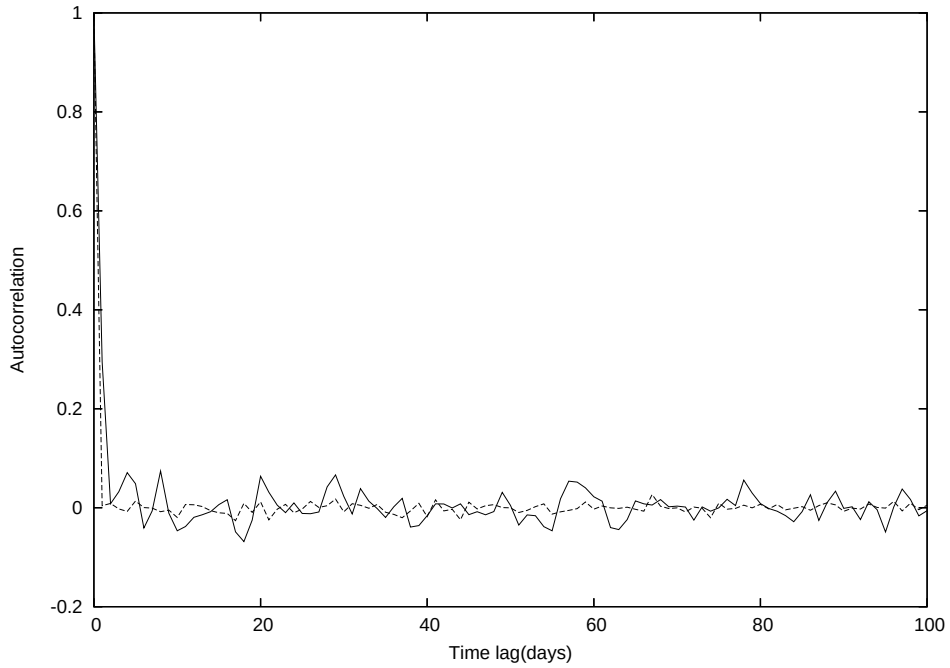

Figure 2.7: The autocorrelation function of S&P 500 daily returns.

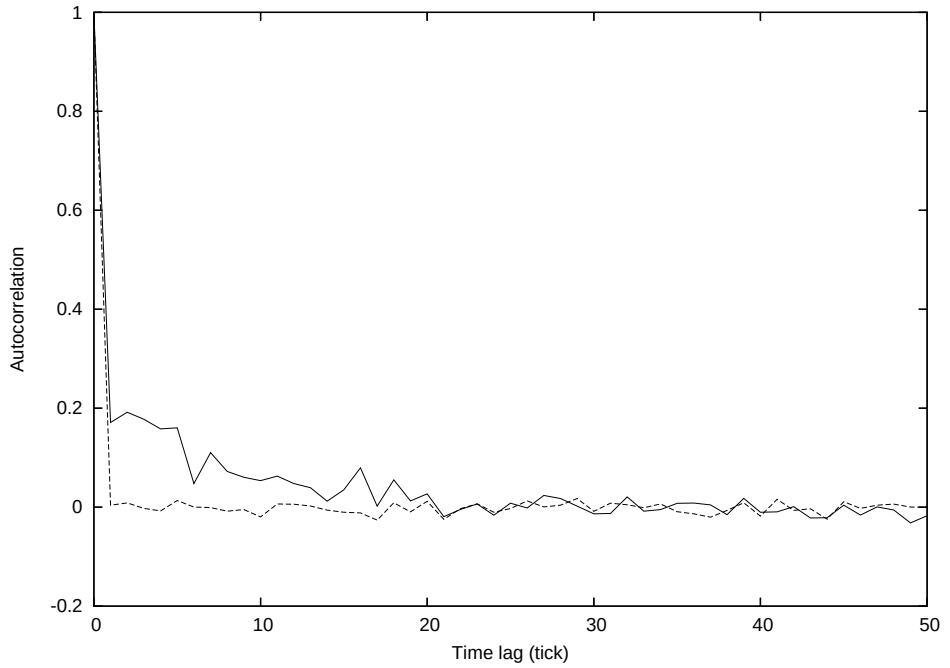

Figure 2.8: The autocorrelation function of S&P 500 tick returns.

2.2.3 Long-term Autocorrelation of Volatility

Short-term autocorrelation in returns does not imply the independence of returns. The latter requires that any non-linear function of return is without

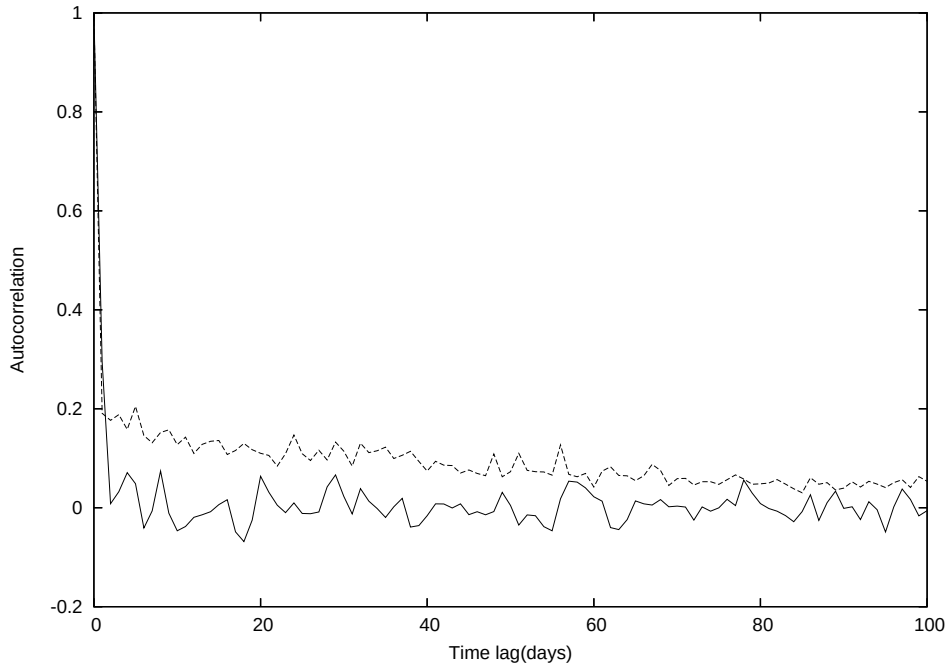

Figure 2.9: Autocorrelation functions of the daily return and the absolute daily return of S&P 500. It shows that absolute values of the daily returns are with long-term temporal correlations.

autocorrelation[8]. Now, let us consider a non-linear function of return, i.e. volatility, which in principle is the standard deviation of the price changes during an appropriate period of time [12].

There are several reasons for considering the statistical properties of volatility:

- Volatility can be directly related to the amount of information arriving in the market;
- Volatility can be directly used in the modeling of stochastic process governing the price changes;
- From a practical point of view, volatility is a key indicator for measuring risk of financial investments [20].

Among the alternative methods to estimate volatility, here we only adopt the absolute return.

The ACF of S&P 500 absolute daily returns is shown in Figure 2.9, together with the ACF of the daily returns. The time range of the data is from January 1970 to September 2004. Long positive autocorrelation of absolute returns can be observed in the plot. In contrast, both the autocorrelations of a set of Gaussian data and that of their absolute values, which are shown in Figure 2.10 (the solid line and dotted line, respectively), immediately drop to the noise

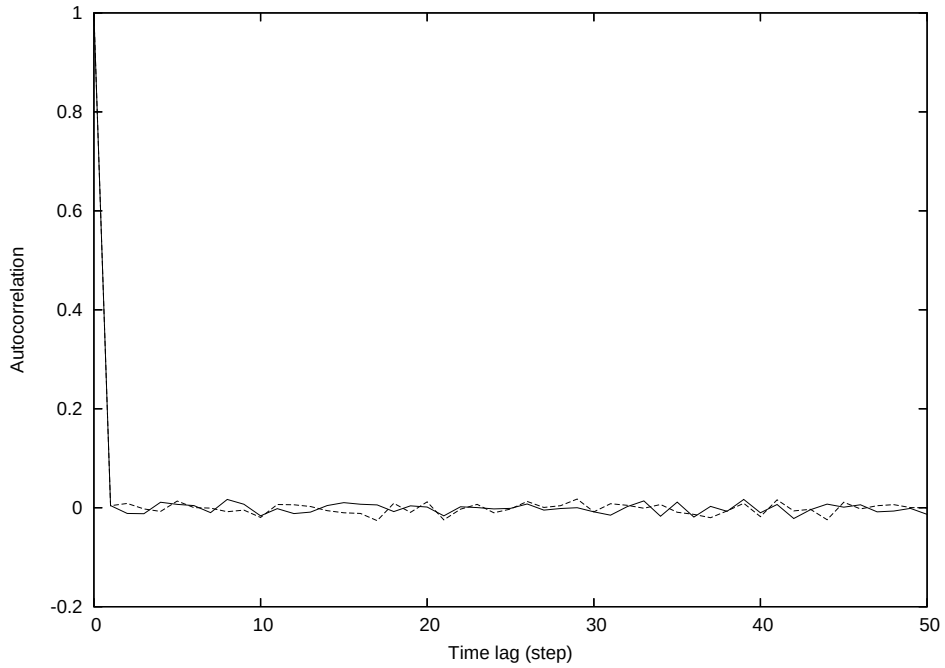

Figure 2.10: Autocorrelation functions of the values and absolute values of a set data following a Gaussian distribution. It shows that no temporal correlations exist in both the values and the absolute values.

range. It implies that there is no temporal correlation in both the data and their absolute values.

The absence of linear correlations and presence of long-time non-linear correlations in returns confirms that the signs of returns are weakly correlated over time, while long time correlations exist in the amplitudes of returns [26].

The long term autocorrelation of volatility is directly related to a characteristic phenomenon — volatility clustering, i.e. "periods of quiescence and turbulence tend to cluster together" [25]. Recalling the return distribution plotted in Figure 2.3, it clearly shows some high returns and that they tends to group together.

Similar stylized facts can be found in different financial time series. Here we further investigate some data of Dow Jones Industrial Average(DJIA) and the exchange rate of Japanese Yen / US Dollar in foreign currency exchange markets.

Figure 2.11 shows the results of DJIA daily data, which were recorded from January 1970 to December 2004. Figure 2.12 displays the stylized facts observed in exchange rate of Japanese Yen/ US Dollar in the same period. Both figures show results similar to that of S&P 500, with respect to the stylized facts.

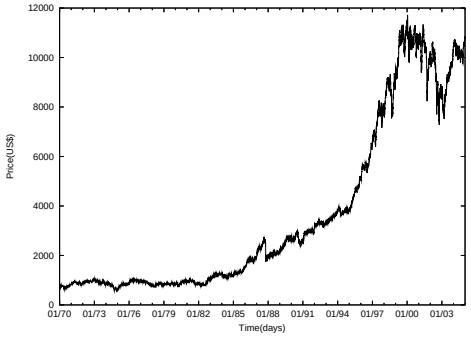

(a) Price.

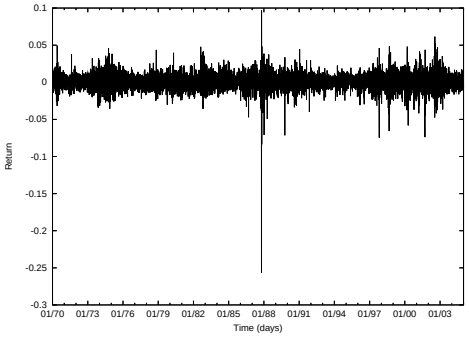

(b) Return.

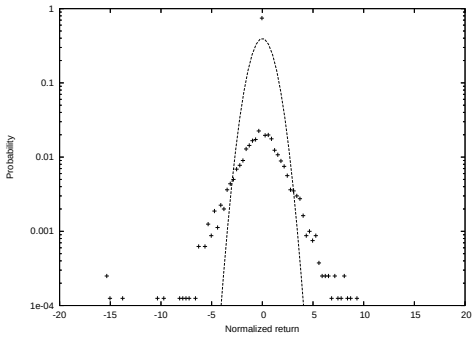

(c) Probability density function.

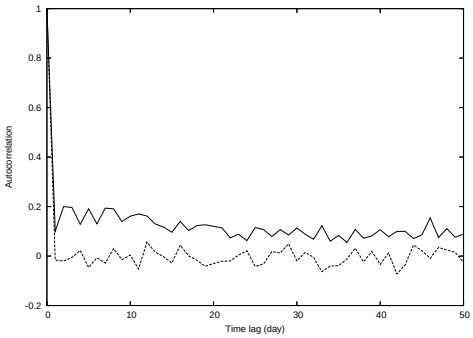

(d) Autocorrelation of return and absolute return.

Figure 2.11: Stylized facts found in Dow Jones Industrial Average Index.

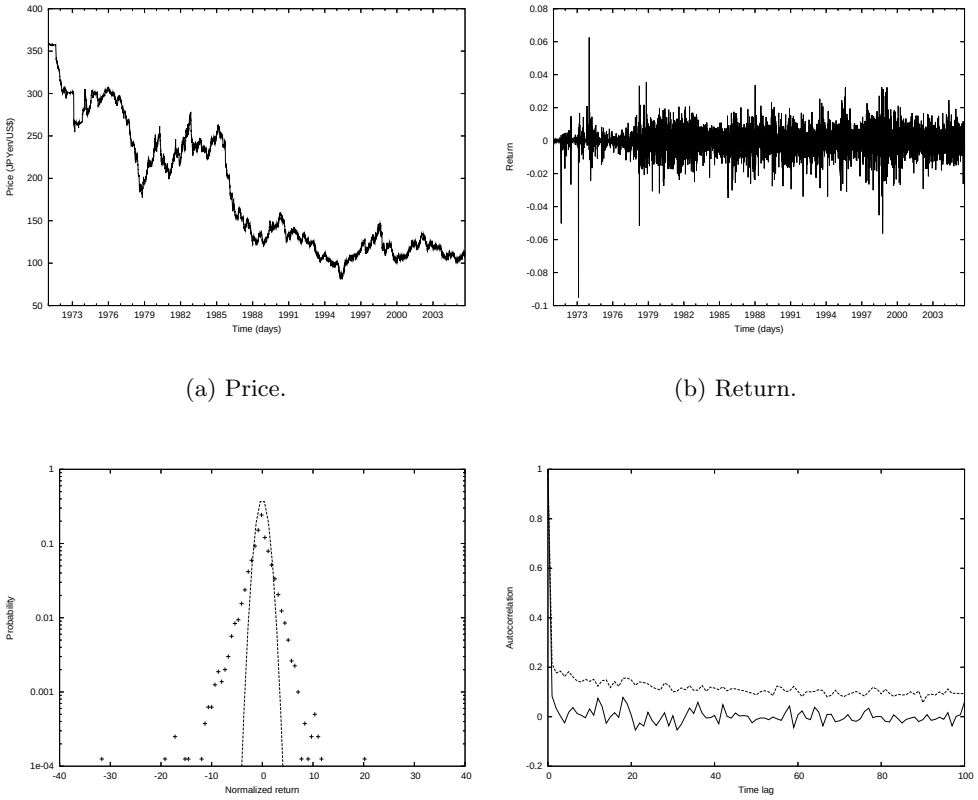

(a) Price.

(b) Return.

(c) Probability.

(d) Autocorrelation of return and absolute return.

Figure 2.12: Stylized facts found in the exchange rate of Japanese Yen/ US Dollar.

As discussed above, the stylized facts of financial time series can not be effectively explained by traditional economic and financial theories. In order to identify the origin of these stylized features, we resort to microsimulation. This is the main theme of this research thesis.

Chapter 3

Microscopic Simulation in General

3.1 The Limitation of the Traditional Methodologies

Traditionally, analytical approaches are commonly used in finance. The methodologies of this type can be further categorized into two classes. One has an econometric character. Here, statistical regression is applied to economic data in order to estimate relationships among different aggregated variables as well as other economic indicators, or to statistically evaluate hypotheses. Predictions can thus be made based on the established theories. The methodology of the other type looks at the feedback between micro-structure and macro-structure. It relies heavily on top-down construction — externally imposed definitions such as fixed decision rule, representative agents and market equilibrium constraints, etc. It ignores the effect of the interaction among the agents [24].

The drawbacks of analytical models have been recognized in three respects [14]. First, most of them rely upon strict assumptions which are often not realistic. For example, many models assume that agents are rational, efficient, homogeneous in type and understand situations analogously. However, experimental studies at least reveal systematic deviations of agents' behaviors from rationality [14]. We can consider this weakness as the price to be paid for the tractability of the models. A specific example for this point is the Black-Scholes equation, which can be solved analytically. The derivation of this option pricing model is based on the assumption that the price of the underlying instrument follows a geometric Brownian motion, transactions are free of costs or taxes, the standard deviation of the underlying asset's returns is known and agreed on by all investors, etc. [12].

Second, analytical approaches such as regression analysis can not isolate cause and effect and therefore their results do not bring any new qualitative understanding of the dynamics under study.

At last, many results generated by analytical models do not agree with empirical data. For example, the GARCH[1] model gives rise to exponential

[1]GARCH stands for generalized autoregressive conditional heteroskedastic, a technique

collapse in autocorrelations of absolute or squared returns, while the decay of empirical autocorrelations follows a power law [7].

The inherent limitation of the traditional methodologies spurs the development of the method of microsimulation in economics and finance.

3.2 The Method of Microscopic Simulation

Microscopic simulation (MS), also known as microsimulation, was first developed in physical sciences as a tool for studying complex systems with many elements, which are generally intractable by analytical methods. The main idea of MS is to model each individual element of the system, and track them and their interactions over time to investigate the behavior of the whole system by simulation. In brief, with MS, we study the complex dynamics of a system from bottom up. In addition to solving problems in physics, MS has been widely applied to study the relation between the microscopic behavior and macroscopic phenomenon in systems in social science, chemistry, biology, etc.

Among many advantages, MS is free of some modeling constraints as described above. Another merit of MS is that it allows us to explore the effect of various parameters. However, for an increasing number of degrees of freedom one might easily generate a parameter space that is not tractable for simulation. Therefore the models should be kept as simple as possible and extra features should only be added if this is necessary [14].

Applications of MS in Finance

Albeit its short history in finance, up till now many MS models have been developed in the finance literature. Most of them focus on the understanding of the complex dynamics of financial markets. These models share some common principles in respect to the modeling of market, agents, interaction between agents and price updating, etc.

Market

Most MS models adopt simple constructions for their models of markets, with one or a few types of agents and one or a few types of financial assets. Some models use a lattice to represent the market, while others model the markets as a pool of agents.

Agent

One distinct advantage of MS is that, in this modeling paradigm, we are much freer to adopt heterogeneous agents. However, there are many MS models based on agents with homogeneous characteristics.

used in finance to model e.g. volatility clustering over time.

Interactions between agents

This aspect of modeling is much diversified among different MS models. For example, different researchers may represent herding behavior in seemingly very different ways. For example, in the model by Bak, herding is denoted as an agent's behavior of drifting his price to the current price or choosing a price of another agent. In the model by Lux, however, herding implies the tendency of agents to follow other agents' who are taking more profitable strategies.

Price formation

Most MS models adopt simple price updating rules, while others use some more involved formula for price formation.

Microsimulation has shown its strengths for studying the complex dynamics of financial markets. This is clear from the fact that many MS models can successfully confirm the main or at least some of the stylized features observed in empirical financial time series. We will describe some of these models in the following chapter.

Chapter 4

Computer Experiments with Three Well-known Models

In this chapter, we will introduce and implement three well-known microsimulation models of financial markets: the Cont-Bouchaud model [6], the model by P. Bak et al. [22] and the model by T. Lux et al. [17] [18]. We will investigate how these models represent real financial markets and agent's behavior, whether they confirm the main stylized facts and what their merits and disadvantages are.

4.1 The Cont-Bouchaud model

4.1.1 Model Description

The market

According to the Cont-Bouchaud model, the market is represented by a pool of N agents whose locations are not important. Instead of grouping traders into a few certain types, as other microsimulation models do, it adopts only homogeneous agents.

The behavior of agents

The agents face three alternatives at each time period: to buy a unit of a financial asset, to sell a unit of asset, or not to trade. Agents tend to form (binary) links between each other with probability c/N. Here c is a connectivity parameter, which represents the willingness of agents to align their actions. The resulting market structure is then described by a *random graph* consisting of N vertices. The connected components correspond to groups of investors. In Figure 4.1, a simple example is shown. These groups decide, independently from other groups, whether to buy, to sell, or not to trade.

According to theoretical analysis [6], when $N \to \infty$ and $c \to 1$, the cluster size distribution follows a power law:

$$P(W) \underset{W \to \infty}{\sim} \frac{A}{W^{5/2}},$$

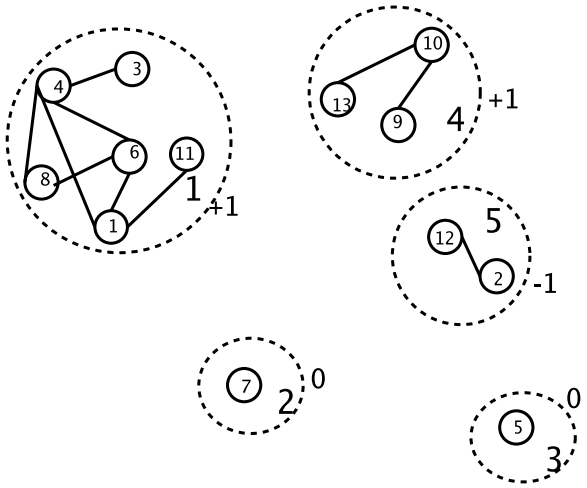

Figure 4.1: An example of a pool of traders consisting of 5 subgroups. $0, -1, 1$ denote the behavior of the different groups, namely remaining inactive, selling and buying, respectively.

where W is cluster size, A is a constant. When c is close to and smaller than 1 ($0 < 1 - c << 1$), the cluster size distribution is cut off by an exponential tail:

$$P(W) \underset{W \to \infty}{\sim} \frac{A}{W^{5/2}} \exp(-\frac{(1-c)W}{W_0}) \tag{4.1}$$

where W_0 is a constant. For the critical value $c = 1$, each agent tends to establish a link with at least another agent.

The demand of a cluster α is denoted as ϕ_α which is equal to 1 for buying, -1 for selling, and 0 for not trading. The variables ϕ are independent with a symmetric distribution: $P(\phi_\alpha = +1) = P(\phi_\alpha = -1) = a$, $P(\phi_\alpha = 0) = 1 - 2a$. The demand of a certain group of traders is proportional to its size.

Price formation

Price change is proportional to excess demand,

$$\Delta p = p(t+1) - p(t) = \frac{1}{\lambda} \sum_{\alpha=1}^{k} W_\alpha \phi_\alpha(t), \tag{4.2}$$

where W_α is the size of cluster α, $\phi_\alpha(t)$ is the individual demand of agents belonging to that cluster, k is the number of clusters, and λ is a so-called market depth parameter which measures the sensitivity of price to changes in excess demand.

In the original paper about the Cont-Bouchaud model [6] a rigorous analytical derivation is given for the cluster size distribution and the distribution of price changes. However, volatility clustering is not considered in the paper.

Furthermore, to the best of our knowledge, no analytical results are known regarding volatility clustering. Therefore, we implemented this model and carried out various numerical experiments. In our implementation we adopted a recursive labeling algorithm to identify clusters.

4.1.2 Simulation Results

From the model description above, it is clear that the cluster formation process is crucial for the price dynamics. From theoretical analysis, it is expected that the cluster size distribution will follow a power law under certain conditions [6]. Figure 4.2 and Figure 4.3 show the cluster size distribution for different values of N when $c = 1$ and $c = 0.8$, respectively. In both experiments the activity parameter is set to 0.001. The dashed line denotes the analytical curve (with $A = 1$ and $W_0 = 0.8$) and the dots represent the estimated probabilities from our simulations. It is clear that the estimated cluster size distribution follows a power law for small values of the cluster size. The range for which the power law is valid becomes wider as the number of agents is increased. The discrepancy between theory and simulations for large values of the cluster size is due to the finite number of agents that are used in the simulations. It should be noted that the analytical expressions are only valid in the limit of infinite number of agents.

Price and price change

Figure 4.4 shows the evolution of the price and the time series of price change[1]. In Figure 4.4(a), there are some large 'jumps' in the price, which correspond to the big 'strokes' in Figure 4.4(b) that reflect large (positive or negative) returns. Due to these large strokes, the probability distribution of price change does not follow a Gaussian distribution. This will be discussed in more detail in the next section.

[1]The Cont-Bouchaud model [6] adopts price change rather than return.

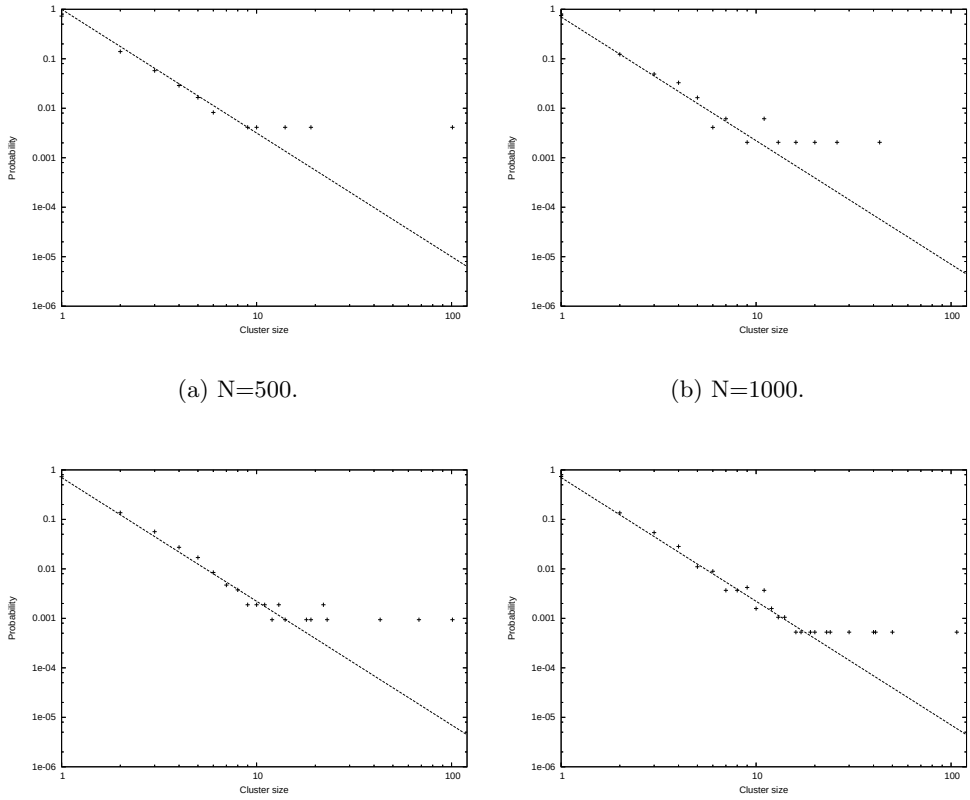

(a) N=500.

(b) N=1000.

(c) N=2000.

(d) N=4000.

Figure 4.2: The cluster size distribution for different values of N, when $c = 1$. The scales of both axes are logarithmic.

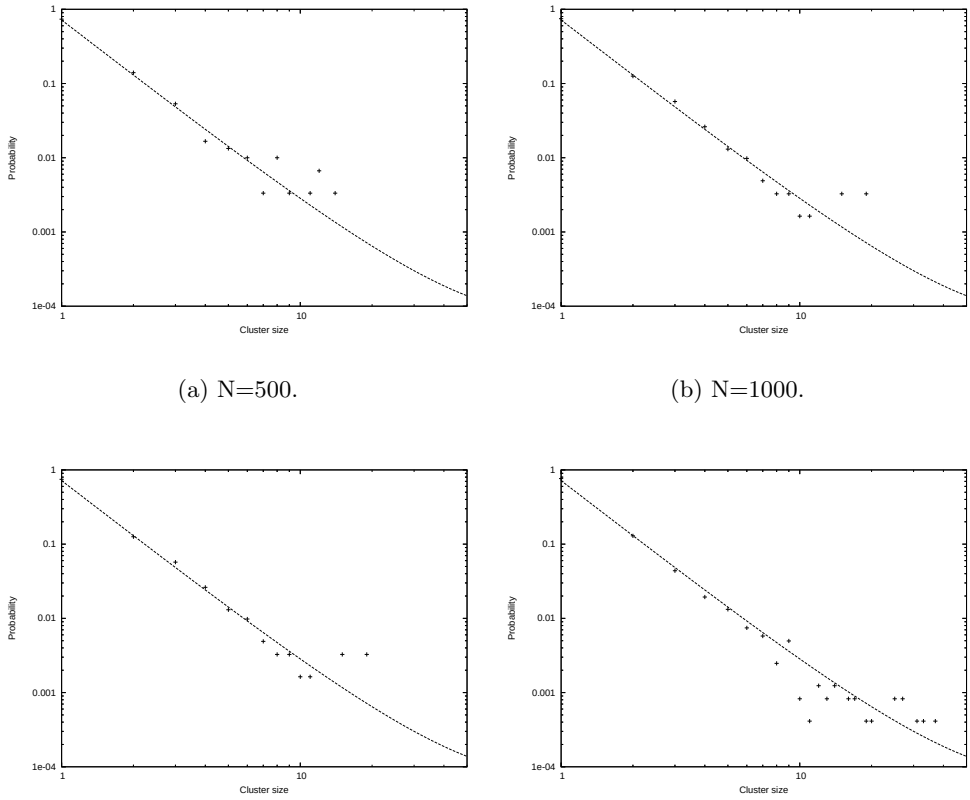

(a) N=500.

(b) N=1000.

(c) N=2000.

(d) N=4000.

Figure 4.3: The cluster size distribution for different values of N, when $c = 0.8$. The scales of the axes are logarithmic.

(a) Time evolution of the price.

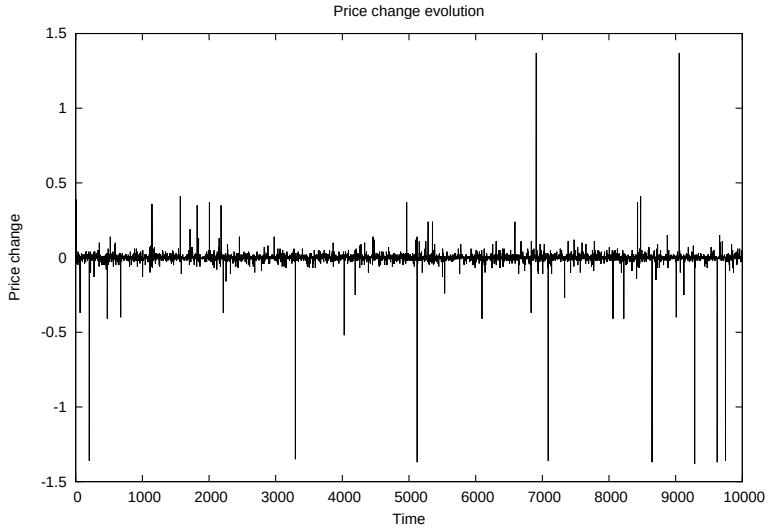

(b) Time evolution of Price change.

Figure 4.4: The evolution of the price and time series of price changes over a time period of 10000 time steps. Here, $N = 1000$, $c = 0.9$ and $a = 0.0005$.

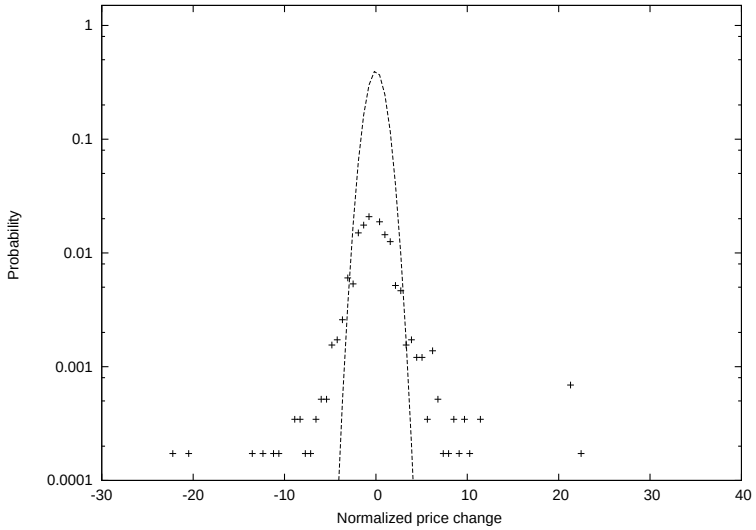

Figure 4.5: Probability distribution of normalized price changes compared with a Gaussian PDF. Here, $c = 0.9$, $N = 1000$ and $a = 0.005$. The scale of the y axis is logarithmic.

Probability distribution of price changes

Figure 4.5 confirms our expectation: "fat tails" can be clearly observed in the histogram of price changes. From the model description above, we can conclude that the large (positive or negative) returns may correspond to the actions of some very large groups. As shown in Figure 4.6, when we decrease the value of c slowly down to 0, meaning that agents are becoming more and more independent, the probability distribution of price change converges to a Gaussian distribution.

We have also performed some investigations with respect to the parameter a. This parameter denotes the activity of agents, and is defined as the probability that agents buy or sell. When $a \ll \frac{1}{2}$ some traders do not participate in trading, while $a \simeq \frac{1}{2}$ indicates the situation that almost all traders are buying or selling. Figure 4.7 shows the probability distributions of price change for different values of a. It can be seen that the smaller the activity is, the fatter the corresponding distribution will be. When $a \simeq \frac{1}{2}$, the distribution is close to a Gaussian distribution. This can be understood as follows: when nearly all of agents are trading, there are no sharp changes in price. Generally these sharp changes are caused by heterogeneities in the demand of the different groups. This is of course connected with the cluster size distribution.

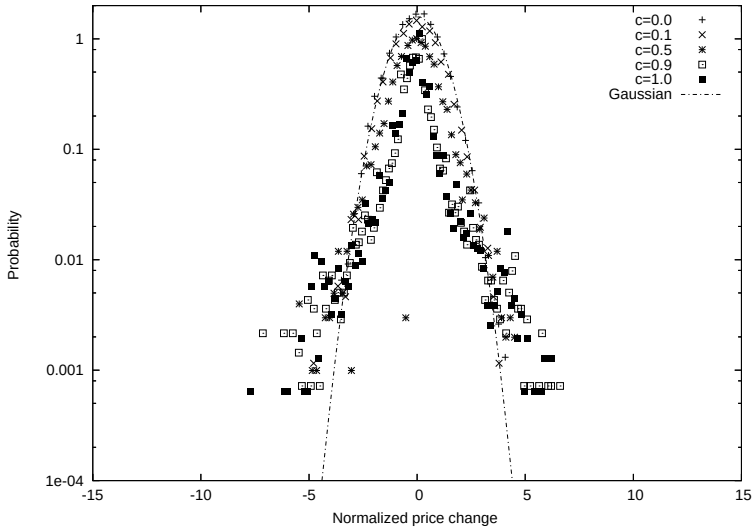

Figure 4.6: The Probability distribution of normalized price changes for different values of c, compared with a Gaussian distribution. Here, $N = 1000$ and $a = 0.005$. For $c \to 0$, a progressive convergence to a Gaussian distribution is observed.

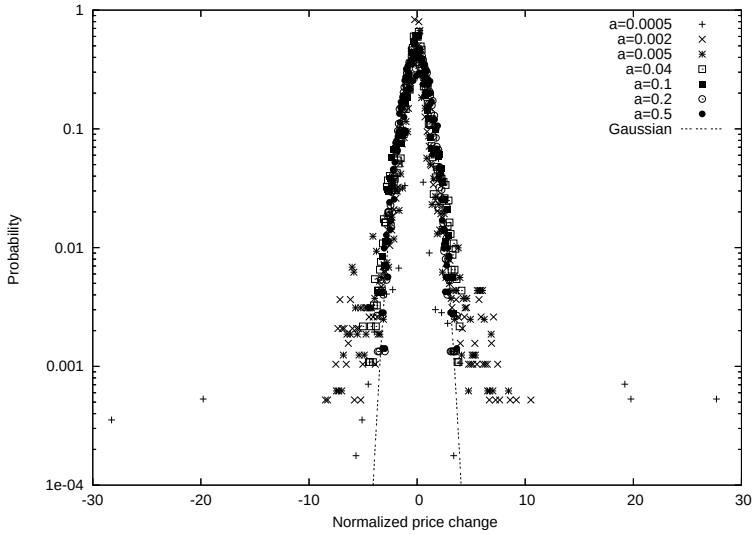

Figure 4.7: The Probability distribution of normalized price changes for different values of the activity parameter a, compared with a Gaussian distribution. Here, $N = 1000$ and $c = 0.9$. For $a \to \frac{1}{2}$, a progressive convergence to a Gaussian distribution is observed.

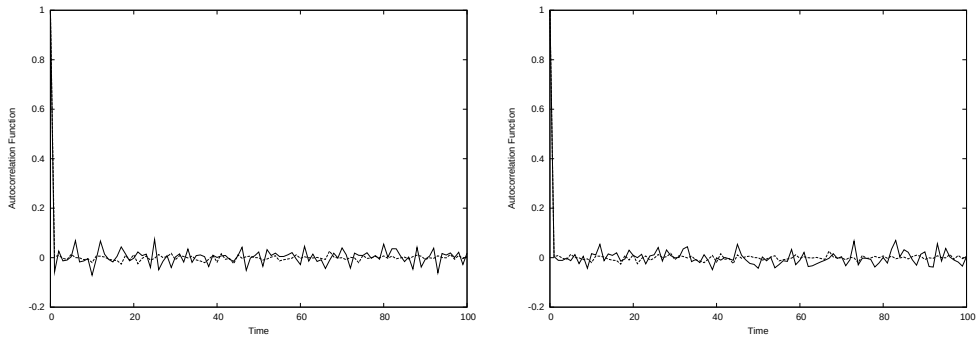

(a) ACF of price changes.

(b) ACF of absolute price changes.

Figure 4.8: Plots of the autocorrelation Function (ACF) of the raw and absolute price changes. Here, $c = 0.9$ and $N = 1000$.

Autocorrelation of price changes and volatility

Next, we consider the autocorrelation of price change and volatility. Similar to our empirical data analysis (see Chapter 2), we will study the ACF of the price change (return) and its volatility. As a comparison, in all figures showing autocorrelation functions, the corresponding ACF of a series of independent normally distributed variables will be included.

Figure 4.8 shows that, when we set the value of c close to 1, the autocorrelation of the price change drops quickly to the noise range. When c is set to other values, we get similar results (see Figure 4.9). The absence of *memory* in price change and in its absolute value is the consequence of the trading behavior of agents: At each time step, if the agents are going to trade, their demands (either $+1$ or -1) are randomly determined. Thus there is no dependence between the demands at any two successive time steps.

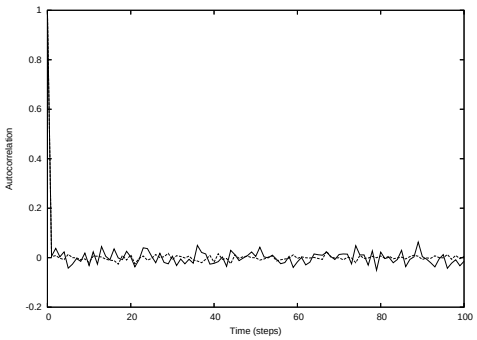

(a) ACF of price changes (c=0.5).

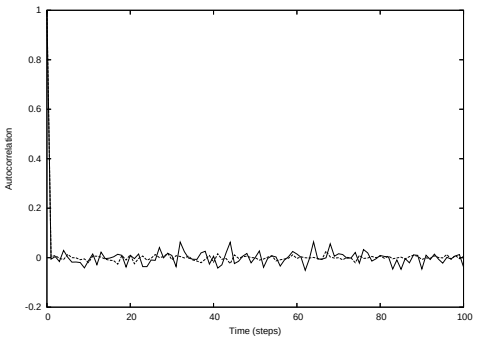

(b) ACF of absolute price changes (c=0.5).

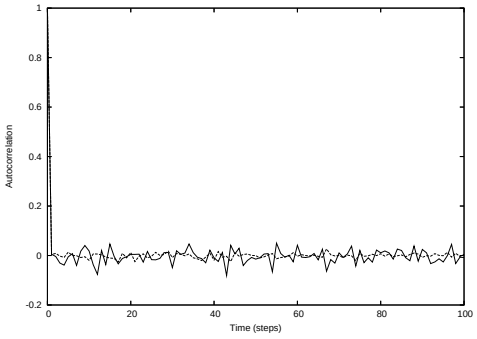

(c) ACF of price changes (c=0.8).

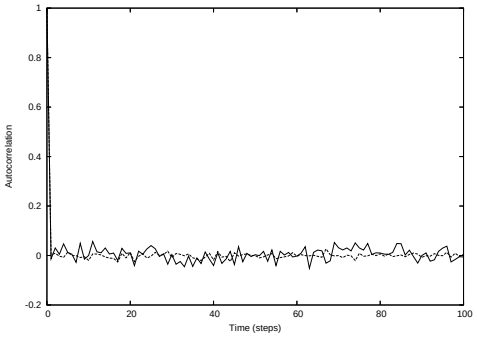

(d) ACF of absolute price changes (c=0.8).

Figure 4.9: Plots of the autocorrelation Function (ACF) of the raw and absolute price changes according to different c value. Here, $N = 1000$.

4.1.3 Discussion

From the discussion above we learn that, according to the Cont-Bouchaud model, (fat-tailed) non-Gaussian distribution is directly caused by heterogeneities in the demand of the different groups and the herding behavior of agents within a group. These heterogeneities are directly connected with the cluster size distribution and the activity parameter. One obvious advantage of this model is that, due to its simplicity, the distribution of return can be solved theoretically. Unfortunately, numerical experiments show that the Cont-Bouchaud model is not able to produce an important stylized fact, namely long term autocorrelation of volatility. During this project, we initiated a subproject with the objective to study the behavior of this model when using a small world network[2] instead of a random graph. The results were similar to what we have reported in this chapter, and more importantly, this modification does not explain volatility clustering [21]. In Chapter 5, we will present a modification of the Cont-Bouchaud model that is able to produce volatility clustering.

4.2 The Model by Bak et.al.

4.2.1 Model Description

The market

According to this model, the market contains of $N/2$ stock shares of only one type. There are totally N agents in the market who are classified into two groups: fundamental value traders and noise traders. Each agent can own at most one share. So at each time step, he can either be a potential buyer or a potential seller of the stock. Each share owner advertises a price at which he is willing to sell his share, and each buyer advertises a price that he is willing to pay for a share. Locations and geographical relations of agents are not considered in this model, *i.e.* interaction can happen between any two agents in the market.

The behavior of agents

According to the model, the biding and asking prices of any fundamental trader and the biding or asking price of any noise trader is initialized in a certain range of values. Fundamental traders choose their prices in order to optimize their utility functions, based on the expected dividends of the company that issued the stock and their risk aversion degrees. Their biding or asking prices will remain the same throughout the simulation, if they do not take participation in trading. As will be discussed below, the price updating mechanism of the noise traders is more versatile. The whole simulation process is composed of a set

[2]Taking a connected graph or network with a high graph diameter and adding a very small number of edges randomly, the diameter tends to drop drastically. This is known as the small world phenomenon. It is sometimes also know as "six degrees of separation" since, in the social network of the world, any person turns out to be linked to any other person by roughly six connections [3].

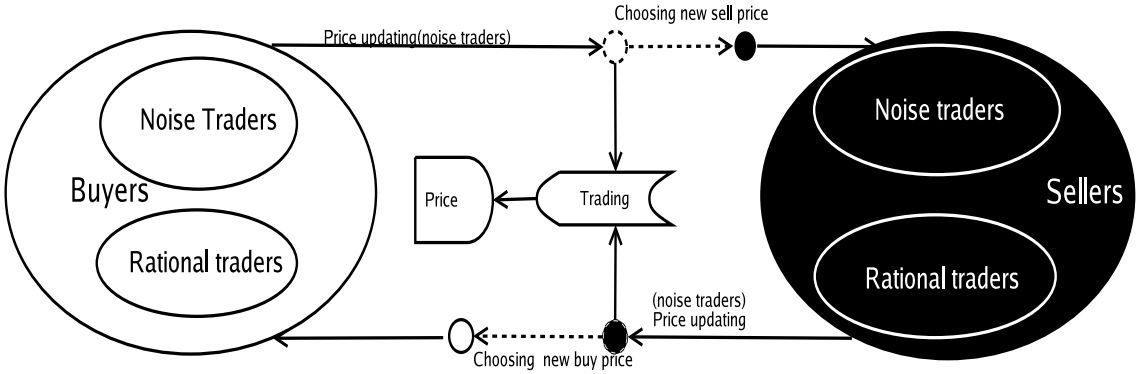

Figure 4.10: Diagram of a trading cycle in the Bak model. Note that if a transaction takes place the status of the trader (buyer or seller) will be switched.

of repetitive trading cycles as shown in Figure 4.10. In each trading cycle, an agent is chosen randomly to perform his operation in the market. Each trading cycle goes through the following three main stages:

1. Before a transaction: The selected agent will update his biding/asking price according to the situation of market and his particular strategy (unless he is a fundamentalist).

2. During a transaction: If there are trading opportunities, he will trade at the most favorite price for him.

3. After a transaction: both traders will exchange their buyer/seller status and choose new biding/asking prices.

The behavior of a fundamental trader is relatively simple, while that of a noise trader, may be quite involved. The latter is defined in the different trading stages during a cycle as follows:

1. In the stage before trading, the price can be updated in two alternative ways:

   (a) the price is changed randomly with equal probability in either the downward or the upward direction. This is similar to the *diffusion* process in physics. The traders who behave in this way are called "independent noise traders".

   (b) The price drifts to the current market price with a probability that is higher than 0.5.

2. In the stage before trading, how strong (in terms of unit) the diffusion or drifting is. There are also two possibilities:

   (a) The strength is one unit.

   (b) The strength is proportional to the actual recent variations of market prices, a feature called 'volatility feedback'.

3. In the stage after trading, how the new initial offering price is set after becoming a new seller (buyer). There are two possibilities here:

   (a) The new asking (bidding) price is determined by randomly choosing a price between the current price and the maximum price (between zero and the transaction price).

   (b) Or by randomly picking a seller (buyer) in the market and copying his price.

To summarize, there are eight ways in which the trading strategy of a noise trader can be modeled.

Price formation

The market price is set to the actual transaction price after each transaction. This is the lowest selling price when a buyer is chosen in the market, or the highest buying price when he is a seller.

4.2.2 Simulation Results

In this section we will present the results obtained in our simulations using different price update mechanism for the noise traders and other parameter settings. We will first show, in the first subsection, the time evolution of price and return. In the next subsection, we will study the distribution of return and the relevant autocorrelation functions following a similar approach as our empirical data analysis as presented in Chapter 2.

Price and return

Let's first suppose that all the agents in the market are rational agents. In Figure 4.11(a) the price evolution corresponding to this case is shown. The initial prices of the fundamental traders are between 50 and 500. It is clear that the price converges to a certain value (around 220) after about 2000 steps. The reason for this is that after a period of trading, no further trade will occur since all the sellers hold the price beyond the market price (220) and all the buyers are waiting to trade at prices below the market price. Figure 4.11(b) gives the snapshots of prices hold by all the agents at different time steps. It confirms that after certain time steps, the buyers and sellers phase separate into non-overlapping regions. In this case, return quickly goes to zero. Clearly this is not realistic.

An interesting question is, how will the market price and return evolve if there are only noise traders? We first consider the situation when all noise traders are independent. Figure 4.12 illustrates the simulation results when we use $N = 500$ independent noise traders with initial prices lower than $p_{max} = 500$. Subfigure 4.12(a) shows the price variation, 4.12(b) shows the snapshots of the selling and buying prices of the traders at different time steps, and 4.12(c) depicts the time series of return. We observe that the behavior of the price and return are not similar to characteristics seen in empirical data. However,

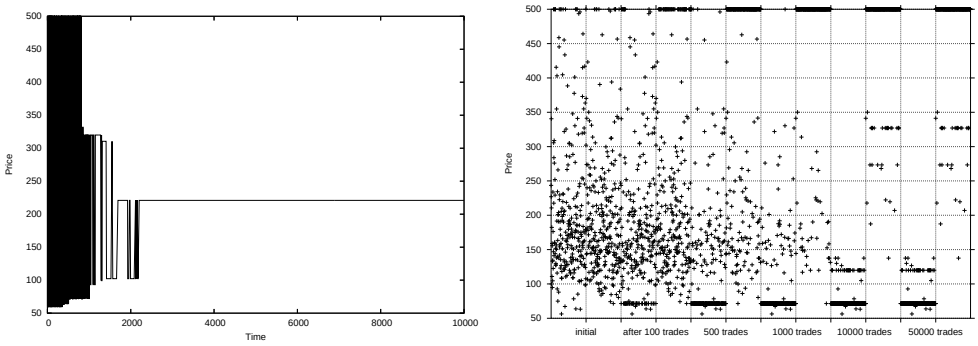

(a) (b)

Figure 4.11: Price evolution when all the agents in market are rational agents. (a) Price evolution. (b) Prices of the agents at selected time steps. Here, $N = 500$, and data for 6 time instances are shown.

some big strokes can be observed in the plot of return which suggests that the distribution of return will not be Gaussian. This will be discussed in more detail in the next section.

In the next experiment the noise traders are allowed to adjust their holding price towards the current market price. A drift coefficient $D = 0.05$ is chosen to determine how strongly the traders want to follow the market price. Time series of the price and return corresponding to this case are shown in Figure 4.13(a) and (b), respectively. We see that there are relatively more big strokes in Figure 4.13(b) compared to Figure 4.12(c). This implies that this type of herding behavior can generate larger variation in return.

Next, another type of herding behavior is added into simulations, namely the so-called "urn" model. After each transaction the agent who had just executed the transaction will randomly pick a buyer or seller in the market and copy his price.

Figure 4.14 shows the simulated prices and returns obtained with the urn model when using $N = 200$ traders. The buying price of each agent $p_b(j)$ is initialized randomly within the range from 1900 to 2000, and the selling price $p_s(j)$ within the range from 2001 to 2100. The highest price is set to $p_{max} = 4000$. It is clear that the price changes more dramatically compared to the previous models. Moreover, it is qualitatively similar to that observed in real markets, e.g. that of S&P 500 (see Figure 2.2). The plot of return does not look similar to that of real data. However, there are still some big strokes which might lead to a non-Gaussian distribution. In addition, it seems that the number of agents does not influence the results very much. The results obtained using 1000 agents are shown in Figure 4.15. It is clear that these are similar to the results obtained with 200 agents. An important feature that we have not seen so far is the volatility clustering phenomenon.

When 'volatility feedback' is added in the "urn" model the results are more

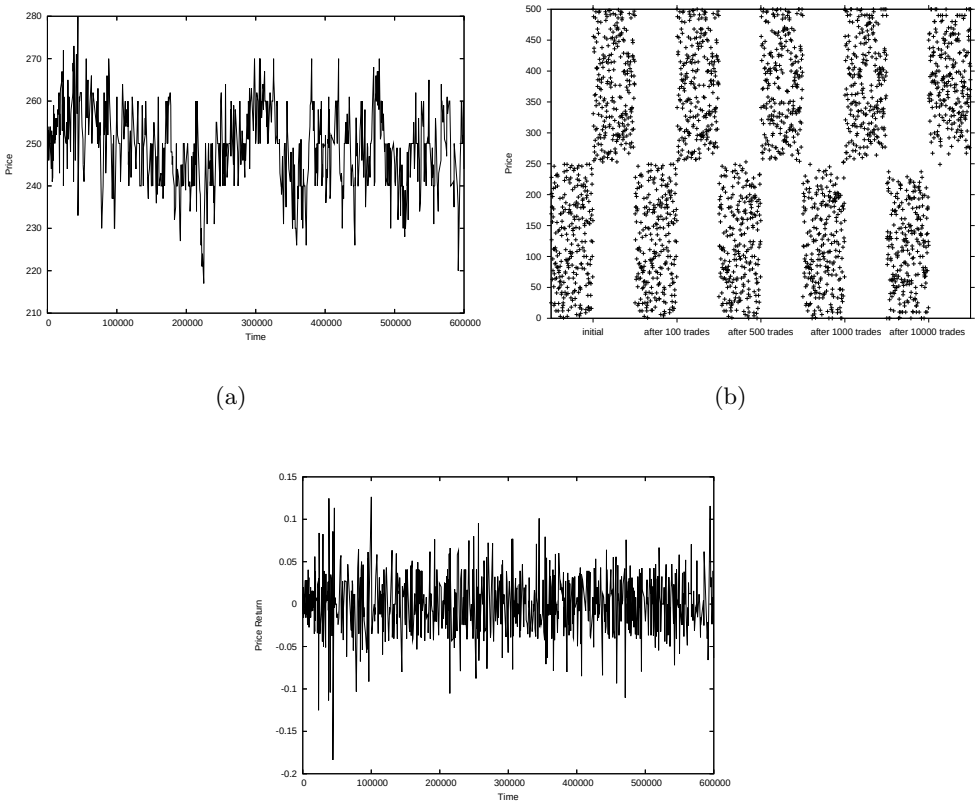

(a) (b)

(c)

Figure 4.12: (a) Price evolution with only independent noise traders. (b) Snapshots of the prices hold by traders at different time steps. (c) Time series of return. Here, $N = 500$, $P_{max} = 500$; all agents in the market are independent noise traders.

realistic. We have carried out experiments using $N = 200$ and $N = 1000$ traders, respectively. Historical prices of 400 time steps are used for calculating the average volatility. By examining the results of both experiments as shown in Figure 4.16(a) and (b), and Figure 4.16 (c) and (d), we conclude that the price evolution obtained with this model is quite similar to that observed in real markets. More importantly, volatility clustering is clearly observed.

In our final simulation with this model, we considered a market consisting of a mixture of rational traders and noise traders. More specifically, we were interested in the effect of the fraction of rational traders (or noise traders) on the time series of price and return. Figure 4.17 shows the simulation results corresponding to different fractions of noise traders: 2%, 20% and 50%. The rational traders' bid and ask prices are initialized in the range from 1960 to 2060. The total number of agents is $N = 1000$.

When there are only 2% rational traders, a few extremely large prices (bub-

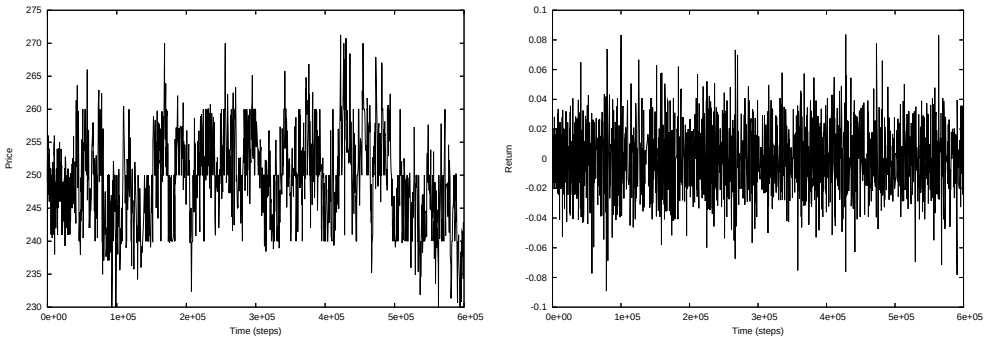

(a) (b)

Figure 4.13: (a) Price evolution when the noise traders drift their biding /asking prices toward the current market price. (b) Price returns. Here, $N = 500$, initial prices of traders are set in the range between 0 and 500.

bles) occur (see Subfigure 4.17(a) and 4.17(b)). When the relative number of rational traders is increased to 20% (see Subfigure 4.17(c) and 4.17(d)), the prices vary within a small range around the fundamental value. This range becomes even smaller when the fraction is further increased to 50%, as shown in Subfigure 4.17(e) and 4.17(f). It is clear that as fraction of rational traders is increased, the market becomes more stable. An overwhelming fraction of noise traders will induce anomalous large price changes. According to this model a behavior similar to empirical data can only be obtained if a small fraction of rational traders is used.

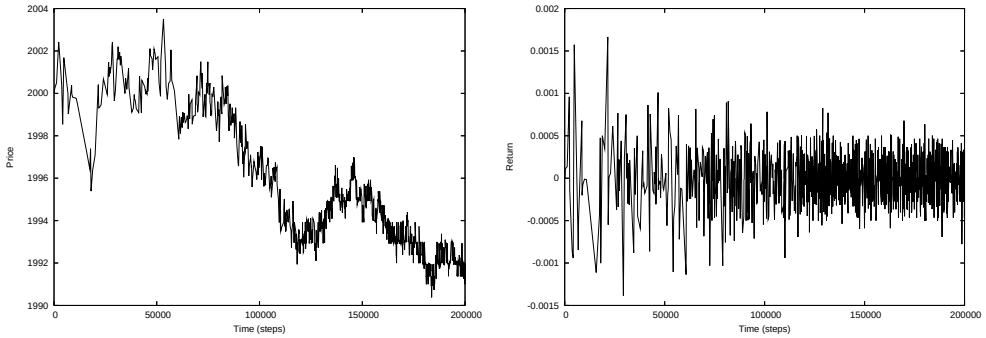

(a) (b)

Figure 4.14: (a) Price evolution of the urn model. (b) Time series of return of the urn model. Here, $N = 200$.

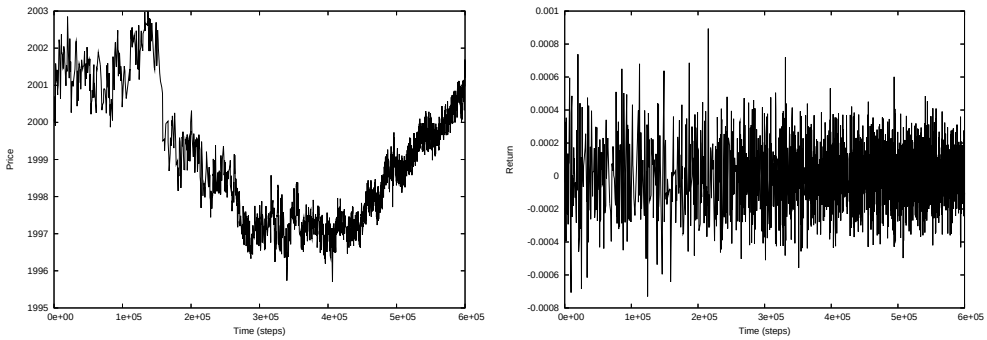

(a) (b)

Figure 4.15: (a) Price evolution of the urn model. (b) Time series of return of the urn model. Here, $N = 1000$.

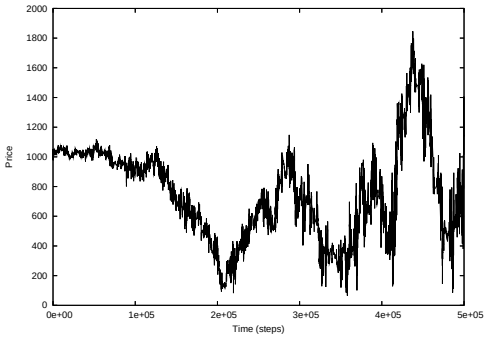

(a) Price, $N = 200$.

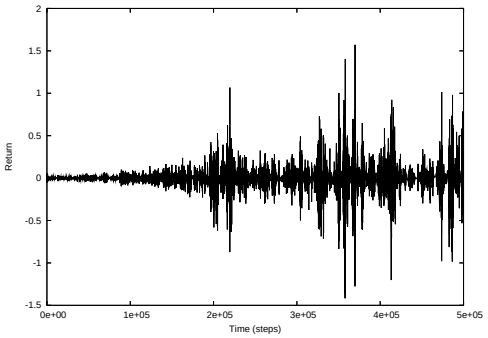

(b) Return, $N = 200$.

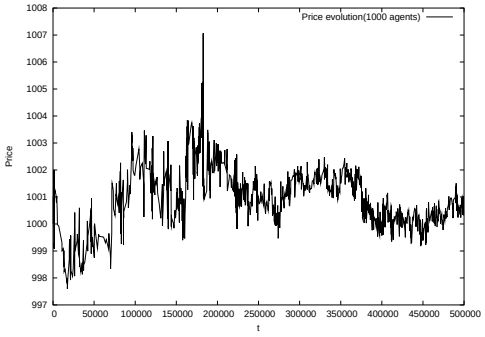

(c) Price, $N = 1000$.

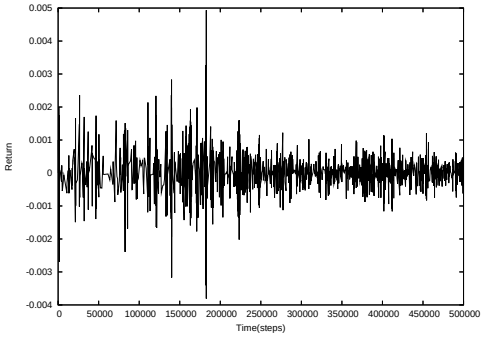

(d) Return, $N = 1000$.

Figure 4.16: Price variations and time series of return, when volatility feedback is added into the urn model. Here, the number of agents are: (a) and (b), $N = 200$; (c) and (d), $N = 1000$.

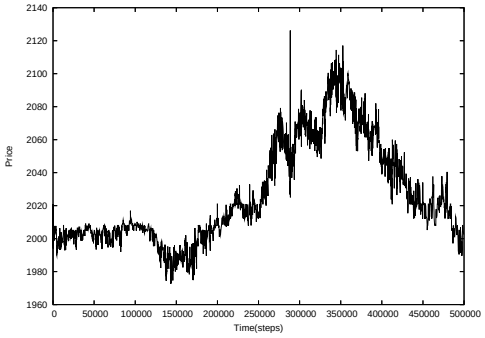

(a) Price, 2% rational traders.

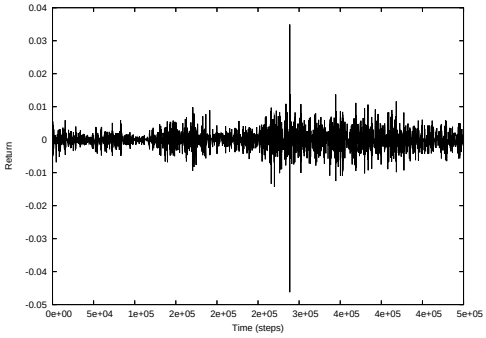

(b) Return, 2% rational traders.

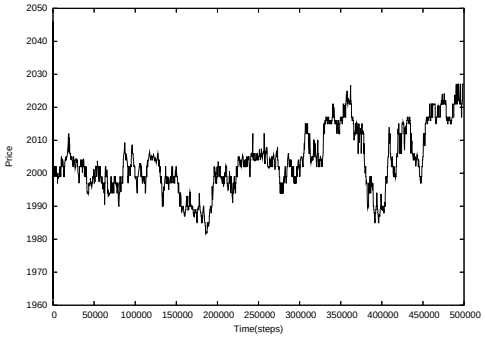

(c) Price, 20% rational traders.

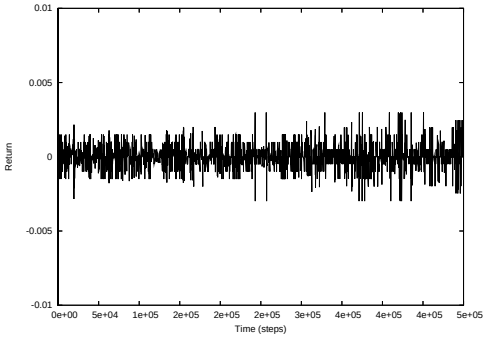

(d) Return, 20% rational traders.

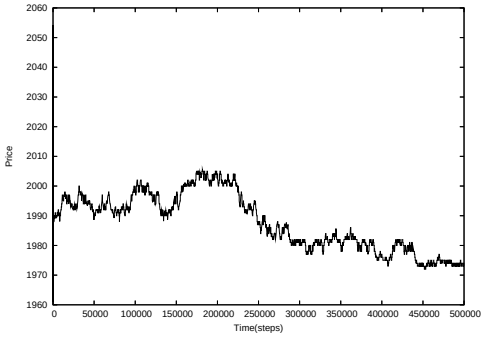

(e) Price, 50% rational traders.

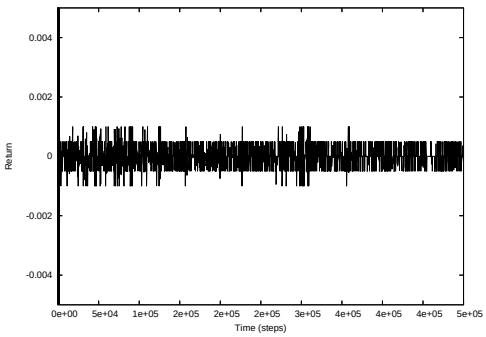

(f) Return, 50% rational traders.

Figure 4.17: Evolution of price and return when the market consists of a mixture of noise and rational traders. Results corresponding to different fractions of noise traders are displayed. (a) and (b): 2%. (c) and (d): 20%. (e) and (f): 50%. Here, the rational traders' asking and biding prices are initialized in the range from 1960 to 2060. The prices hold by noise traders are initialized within the range from 1800 to 2200. The number of agents is $N = 1000$.

Type of trades	Kurtosis
100% noise traders (independent)	3.6143
100% noise traders (drifting to market price)	4.7434
100% noise traders (urn)	6.0847
100% noise traders (urn with volatility feedback)	248.2751
Mix type 2% rational traders (urn with volatility feedback)	209.7075
Mix type 20% rational traders (urn with volatility feedback)	104.08
Mix type 50% rational traders (urn with volatility feedback)	12.23

Table 4.1: Kurtosis of the time series obtained using different fractions of rational traders and different models for the behavior of the noise traders.

Probability distribution of return

In the previous subsection we have presented the time series of price and return for different strategies employed by the noise traders and market scenarios. Here we will study the probability density function of return and the autocorrelation function of return and volatility for the corresponding cases.

When a market consisting of only rational traders is considered, we have seen that the price converges quickly to a constant level. Obviously the return is simply zero for most of the time.

Figure 4.18 shows the PDFs of the normalized return when considering a market with only noise trades. We consider four different strategies for the price updating, namely a random price adjustment, a price drifting towards the current market price, a strategy following the 'urn' model, and a strategy following the 'urn' model with volatility feedback. As the model is refined, we clearly see that the PDF becomes non-Gaussian.

In the previous chapter we have seen that the Cont-Bouchaud model ascribes the 'fat-tailed' distribution to the "herding behavior". From the experiments with Bak's model, we have found that 'fat-tailed' distribution of return can be generated when herding is included as is the case in the 'urn' model. The PDF then is clearly non-Gaussian. However, when a model is used with based on a drift towards the market price, fat tails are also observed. We believe that due to the drifting of the price towards the market price, an indirect herding mechanism is introduced. It should be noted that the current market price is the price at which a trade was executed in a previous time step. This of course is a price that a seller or buyer was holding. By drifting towards this price the behavior of that specific trader is mimicked to some extend. When only diffusion is considered, the distribution does not deviate significantly from a Gaussian distribution. In Table 4.1 the kurtosis of the time series of return are presented for the different cases. When a herding mechanism is present the Kurtosis is significantly greater then 3. As expected when volatility feedback is included, the kurtosis is much higher compared to the cases without volatility feedback. If in addition, rational traders are included, the kurtosis decreases. This is expected because the rational traders tend to stabilize the market.

We further investigate the impact of the volatility feedback. Figure 4.19

shows the PDFs of return when using various lengths for the time window that is used to calculate the average volatility. It is evident that the longer the time window is, the stronger the PDF deviates from the Gaussian distribution. This can be understood by looking at the time series of the return (see Figure 4.15). It is clear that as the time window is increased to 3000 time units, the more volatile the behavior within the time window is.

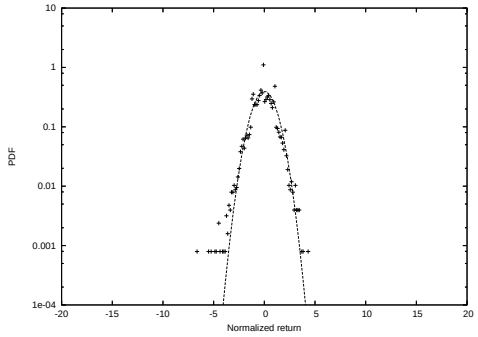

(a) Independent noise traders.

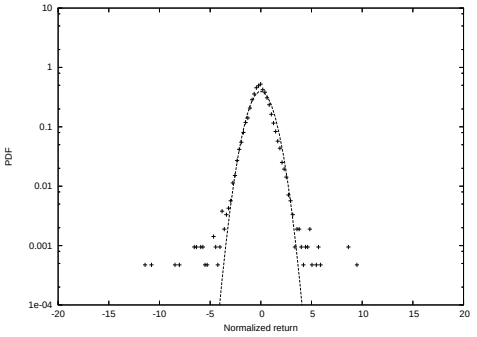

(b) Drifting to market price.

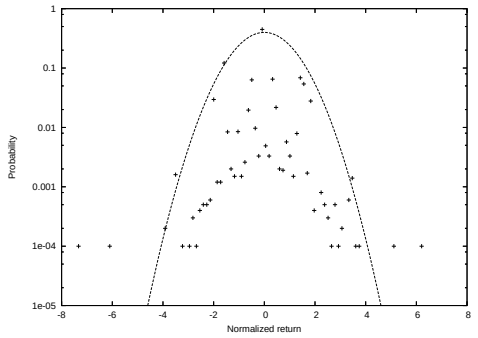

(c) According to the "urn" model.

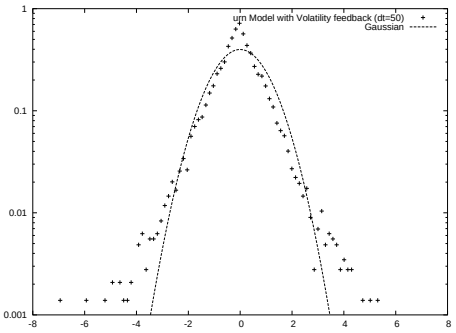

(d) According to the "urn" model with volatility feedback.

Figure 4.18: Probability density function corresponding to the following cases: (a) Model with independent noise traders only. (b) Model with noise traders who drift their price towards the current market price. (c) Model with noise traders who follow the 'urn' model. (d) Model with noise traders who follow the 'urn' model with volatility feedback. Here, $N = 1000$, and a market with only noise traders is considered.

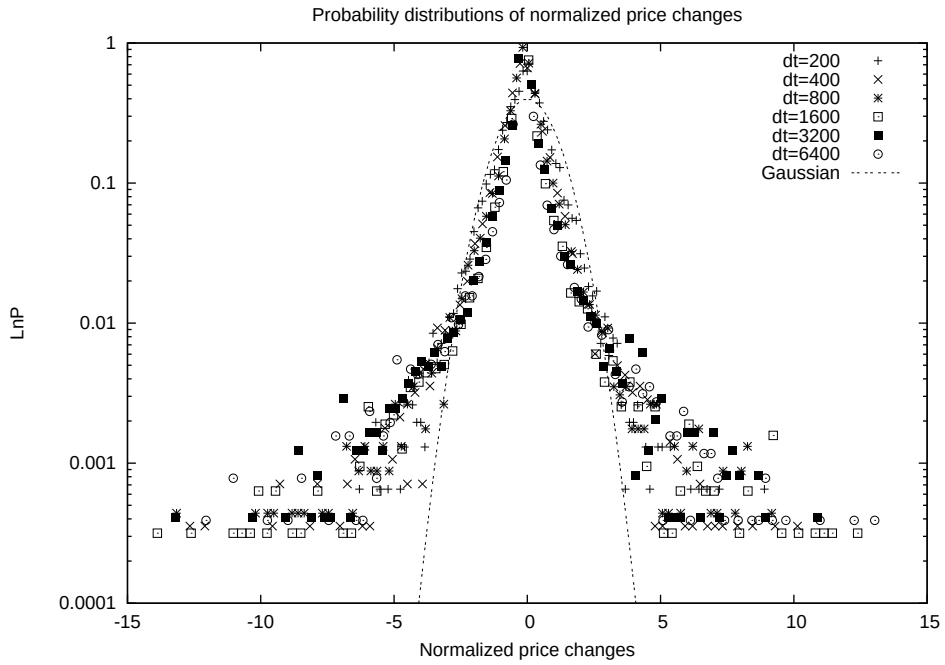

Figure 4.19: Return distributions of the cases with volatility feedback added into the model. Different lengths of memory time are used here.

Autocorrelation of return and volatility

In the remainder of this section we will focus on the autocorrelation of return and absolute return. In Figure 4.20 the ACF of return and that of absolute return are shown for the different cases considered above. We see that the ACF decays quickly to the noise range when a model is used with only independent noise traders or with noise traders using a drifting mechanism or with noise traders mimicking the 'urn' behavior. When volatility feedback is introduced into the model a long term decay of the ACF of absolute return is observed. This is expected because in that case the volatility clustering effect was clearly observed in the time series of return.

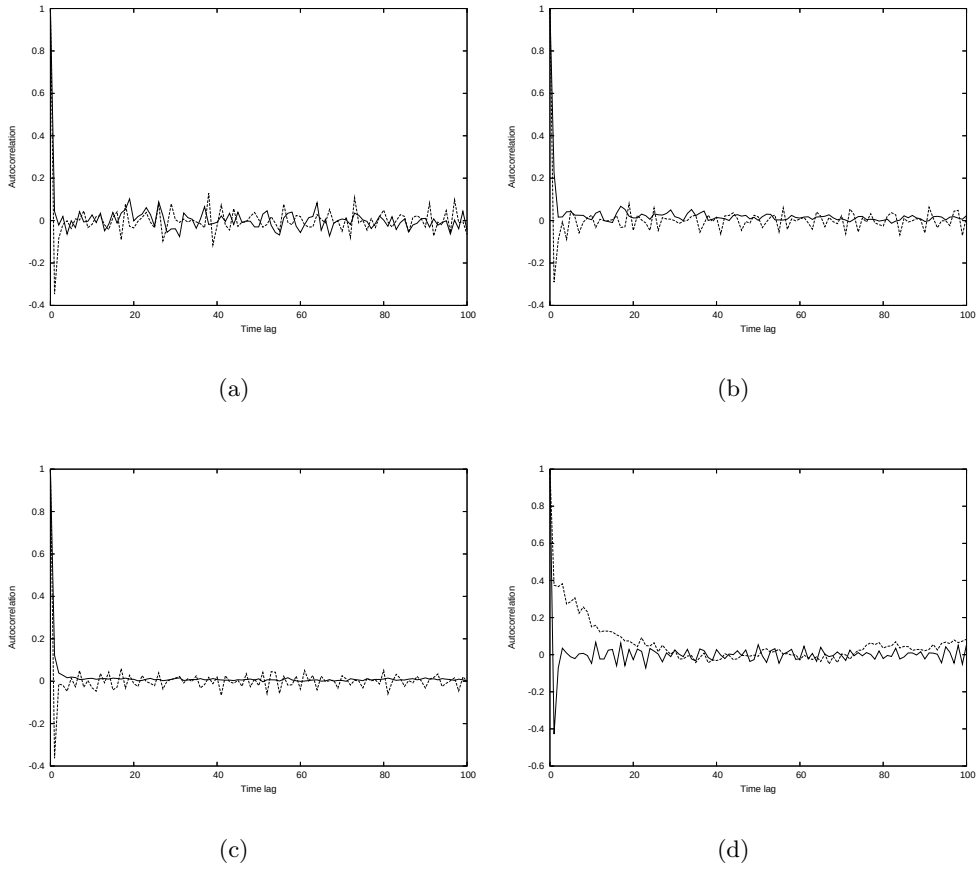

Figure 4.20: ACF of raw and absolute return obtained using Bak's model with different types of traders. (a) Independent noise traders. (b) Noise traders with drifting behavior. (c) Noise traders with 'urn' behavior. (d) Noise traders with 'urn' behavior and volatility feedback.

Finally, in Figure 4.21, the ACF of return and that of absolute return are shown when using different fractions of rational traders in a model where the noise traders follow the 'urn' behavior with volatility feedback. In Figure 4.21(a), we see that the autocorrelations of return quickly drop to the noise

range for all cases. Figure 4.21(b) shows that the corresponding autocorrelations of volatility have different lengths of memory. The top curve is the ACF of absolute return corresponding to a fraction of 2%, the middle one corresponding to a fraction of 20% and the lowest one corresponding to a fraction of 50%. This implies that the noise traders tend to amplify the effect of volatility clustering.

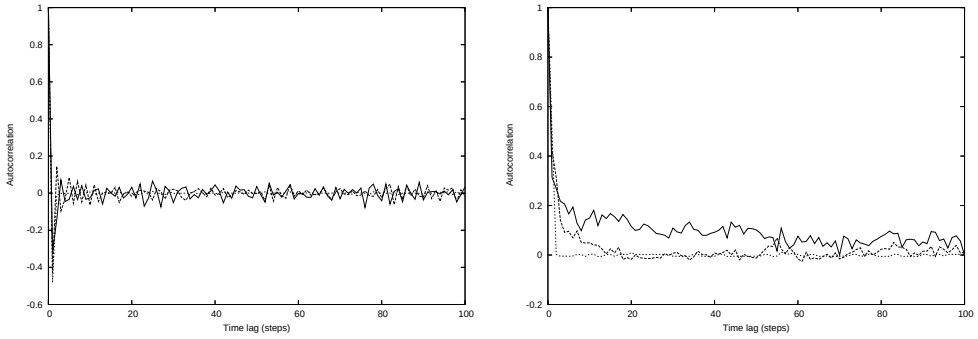

(a) (b)

Figure 4.21: (a). ACF of return when the market consists of a mixture of rational and noise traders. (b) The corresponding ACF of absolute return.

Similar to what we have done above (see Figure 4.19), we show the ACFs when different time windows are used to calculate the average volatility. Here, the parameter setting is the same as that used for Figure 4.18. The results are depicted in Figure 4.22. It is shown that for increasing length of the time window, the ACF of absolute return decays slower.

4.2.3 Discussion

This model is based on rational and noise traders. The strength of the imitating behavior depends on the fraction of rational traders and on the model that is used for the price updating of the noise traders. If this fraction is high the market will be more stable. Conversely, if the fraction of noise traders is high, large price variations might occur. While the 'diffusion' behavior of noise trader can barely generate non-Gaussian distributions of return, it is the behavior of imitation or herding that accounts for distinct 'fat-tailed' distributions. Volatility feedback is responsible for the phenomenon of volatility clustering: the historic price does influence the current or future return.

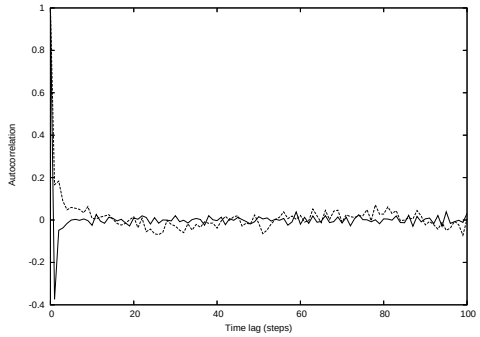

(a) dt=200.

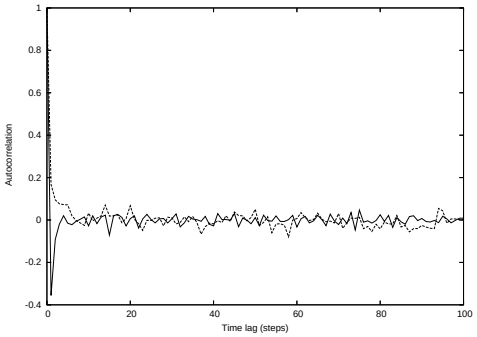

(b) dt=400.

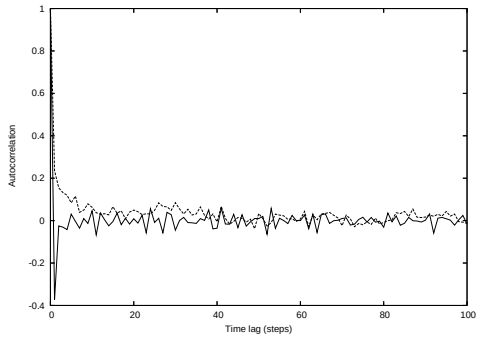

(c) dt=800.

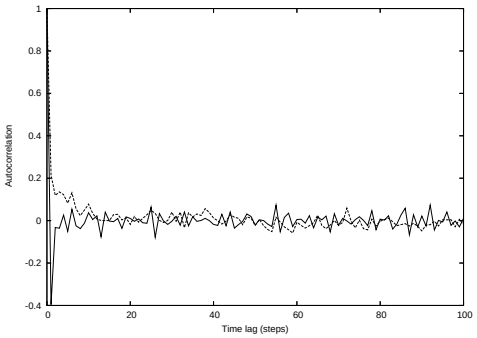

(d) dt=1600.

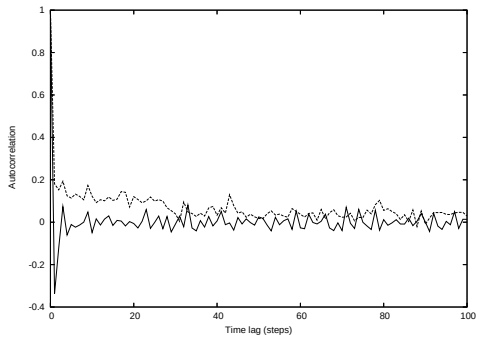

(e) dt=3200.

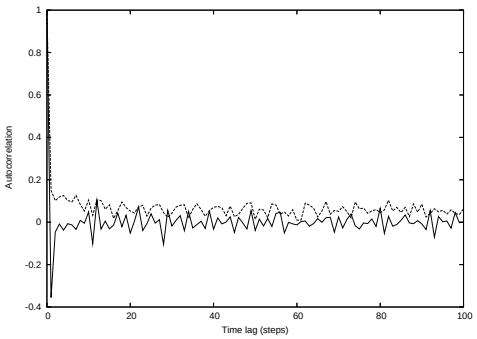

(f) dt=6400.

Figure 4.22: ACF of return and absolute return for the cases when volatility feedback is added into the model. Different lengths of the time window are used here for comparison. Here, 1000 noise traders are used.

4.3 The Lux-Marchesi Model

4.3.1 Model description

The market

The Lux-Marchesi model [15, 16, 17, 18] uses two types of agents: Fundamentalists and chartists. Chartists are further divided into optimists and pessimists. Optimists will always buy units of asset, while pessimists will always sell units of asset. Fundamentalists look at the fundamental value of the stock (p_f), and buy (sell) if the actual market price (p) is below (above) the fundamental value. Contrarily, chartists look at the present *price trend* on the market and the behavior of other agents, rather than the fundamental value.

Agent behavior

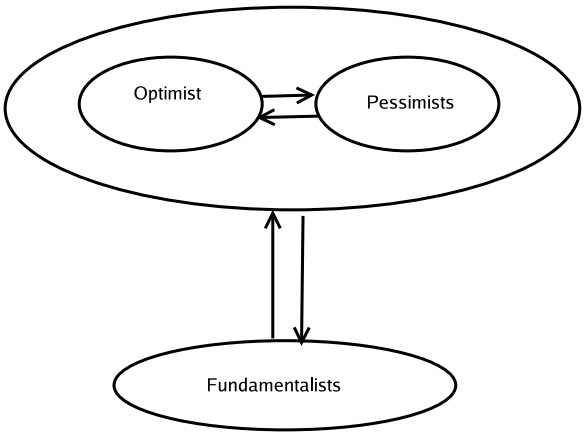

Figure 4.23: Diagram of the Lux-Marchesi model.

The key feature of the Lux-Marchesi model is the movement of agents among different groups or equivalently, the switching of traders to different trading strategies. Figure 4.23 illustrates the switching scheme which consists of following possibilities:

1. Movements between optimists and pessimists.

   Switches of noise traders between the optimistic strategy and the pessimistic strategy are dependent on the combined effect of the majority opinion of all noise traders which is referred as the *flow* and the prevailing price trend which is called *chart*. The former is represented by *opinion index* x, which is defined as

   $$x = \frac{n_+ - n_-}{n_c}, \tag{4.3}$$

   where n_+ is the number of optimistic chartists, n_- is the number of pessimists and $n_c = n_+ + n_-$ is the number of chartists.

The latter is expressed as $\frac{\dot{p}}{v_1}$, here p is the price, $\dot{p}= \frac{dp}{dt}$ (the price change), v_1 is a parameter that denotes the frequency of revaluation of opinion.

The transition probabilities of chartists are described as follows:

$$\pi_{+-} = v_1(\frac{n_c}{N}exp(U_1)) \quad (4.4)$$

$$\pi_{-+} = v_1(\frac{n_c}{N}exp(-U_1)) \quad (4.5)$$

$$U_1 = \alpha_1 x + \alpha_2 \frac{\dot{p}}{v_1}$$

where N is the total number of traders; α_1 and α_2 are, respectively, the parameters measuring the importance that the individuals place on the majority opinion and the actual price trend in forming expectations about future price changes; π_{+-} is the probability of pessimists switching to optimists , and π_{-+} is the probability of optimists switching to pessimists.

This equation implies that the possibility of changing to another strategy becomes higher when the actual movement of price is in a direction which is in contradiction to a trader's own expectation.

2. Movements between fundamentalists and chartists

   Movements between noise traders and fundamentalists are triggered by the comparison of the excess profits from their respective strategies. Generally, traders will move to the more successful group. Specifically, transition probabilities relies on *pay-off differential*, the net gain from one investment after the deduction of the gain that would have received from other investment. The gains of the traders of various types are shown here.

   (a) The gain expected by fundamentalists is

   $$s|\frac{p_f - p}{p}|,$$

   where p_f is the fundamental value, p is the price, $s < 1$ is a discount factor because a gain will only be realized after the price reverses to the fundamental value.

   (b) The gain of optimists is

   $$(r+ \dot{p})/p,$$

   here r is the nominal dividend of the asset.

   (c) The gain of pessimists is R, the average real return from other investments.

Then, by considering the opportunity costs[3], the pay-off differential of the strategy of optimists is

$$((r + \frac{\dot{p}}{v_2})/p - R - s|\frac{p_f - p}{p}|),$$

and that of the pessimists is

$$(R - (r + \frac{\dot{p}}{v_2})/p - s|\frac{p_f - p}{p}|),$$

where v_2 is a parameter for the frequency of this type of transition.

Consequently, the transition probability from fundamentalists to optimists π_{+f} and *vice versa* π_{f+}, from fundamentalists to pessimists π_{-f} and *vice versa* π_{f-}, respectively, are described by the following set of equations:

$$\begin{aligned}
\pi_{+f} &= v_2(\frac{n_+}{N}exp(U_{2,1})), && (4.6)\\
\pi_{f+} &= v_2(\frac{n_f}{N}exp(-U_{2,1})), && (4.7)\\
\pi_{-f} &= v_2(\frac{n_-}{N}exp(U_{2,2})), && (4.8)\\
\pi_{f-} &= v_2(\frac{n_f}{N}exp(-U_{2,2})), && (4.9)\\
U_{2,1} &= \alpha_3((r + \frac{\dot{p}}{v_2})/p - R - s|\frac{p_f - p}{p}|),\\
U_{2,2} &= \alpha_3(R - (r + \frac{\dot{p}}{v_2})/p - s|\frac{p_f - p}{p}|).
\end{aligned}$$

where α_3 is a measure of the pressure exerted by profit differentials.

Price formation

The prices are adjusted by an auctioneer (market maker) in balancing demand and supply. The aggregate excess demand is $ED = (ED)_c + (ED)_f$, where $(ED)_c$ and $(ED)_f$ are the excess demands of chartists and fundamentalists, respectively. Since all chartists either buy or sell the same number t_c units, $(ED)_c = (n_+ + n_-)t_c$. Depending on the deviation of the price from the fundamental value, reaction strength γ and number of fundamentalists n_f, the excess demand of fundamentalists is given by $ED_f = n_f\gamma(p_f - p)$. Assuming that there are additional liquidity traders in the market whose excess demand is stochastic or that the value of aggregate excess demand is perceived with some imprecision by the auctioneer, the model further adds a (small) noise term μ that follows a Gaussian distribution with mean 0.0 and standard deviation $\sigma = 0.05$. Then

[3] rate of return that a business could earn if it chooses another investment with equivalent risk.

the transition probabilities for an increase or decrease of the market price by a fixed amount $\delta p = \pm 0.01$ is expressed as

$$\begin{aligned} \pi_{\uparrow P} &= max[0, \beta(ED + \mu)] \\ \pi_{\downarrow P} &= -min[0, \beta(ED + \mu)] \end{aligned} \tag{4.10}$$

where β is a parameter for the reaction speed of the auctioneer.

Another stochastic factor can also be embedded into the fundamental price, by assuming that changes of the (log) fundamental value follows a Wiener process: $ln(p_{f,t}) = ln(p_{f,t-1}) + \epsilon_t \Delta t$ with $\epsilon_t \sim N(0, \sigma_\epsilon)$. In our experiments, we assume $\sigma_\epsilon = 0.005$ [18].

4.3.2 Simulation Results

Figure 4.24 shows the time evolution of price, return and the fraction of chartists z, when the μ is adopted as the only source of noise. The parameter set is: $N = 500$, $v_1 = 3$,$v_2 = 2$, $\beta = 6$, $T_c(\equiv Nt_c) = 10$, $T_f(\equiv N\gamma) = 5$, $\alpha_1 = 0.6$, $\alpha_2 = 0.2$, $\alpha_3 = 0.5$, $p_f = 10$, $r = 0.0004$, $s = 0.75$.

When we only take the uncertainty in the fundamental value, similar results are obtained as shown in Figure 4.25. Here, 80% of the traders in the market are fundamentalists, and 20% are chartists. The parameters setting is the same as the ones used above.

The simulation results when we adopt both types of noise simultaneously is displayed in Figure 4.26. Same parameters are again used.

Price and return

In the plots of price in both figures, we notice that some very large events happen and they tend to occur together. Correspondingly, some very large returns and clusters of larger returns are clearly shown in the plots of return. In addition, we see that fluctuations of return are remarkably correlated with the changes of the fraction of chartists — z. This correspondence provides a clue to the cause of volatility clustering: If the market is with a high fraction of fundamentalists, the market will move strongly towards the fundamental equilibrium. When the market is under the dominance of the chartists' practice, deviations from the fundamental equilibrium become self-reinforcing and the system can no longer maintain its local stability.

In the case that both noises are present at the same time, we see that the plots of price and return are more similar to the ones shown in Figure 4.25. Therefore, it seems that the noise in the fundamental value has a stronger impact on the dynamics than the noise in the process of price adjustment, provided that they have the same standard deviation.

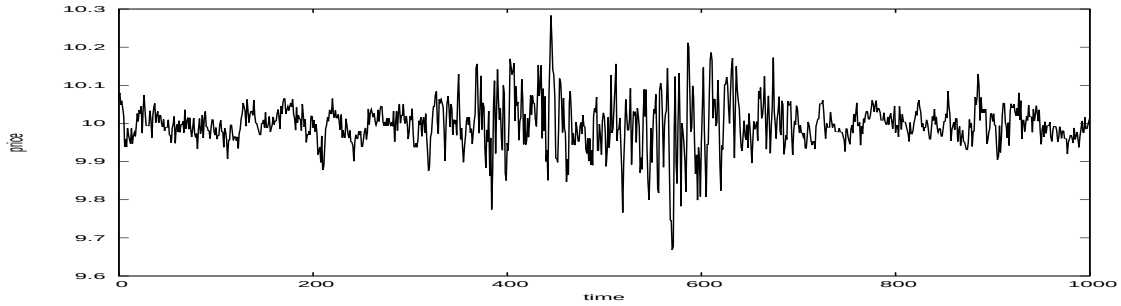

(a)

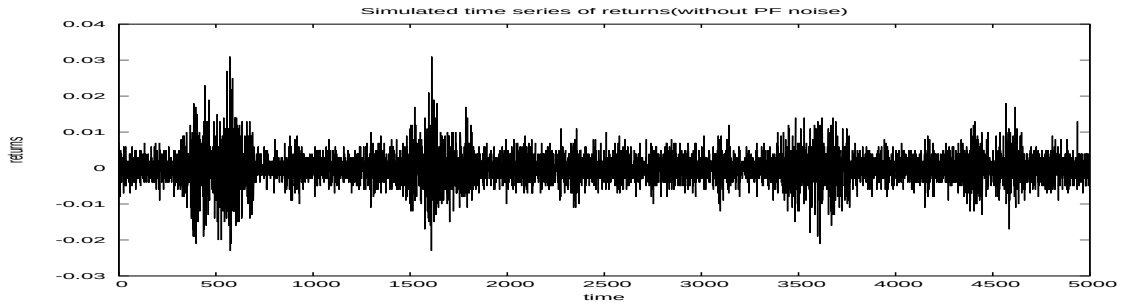

(b)

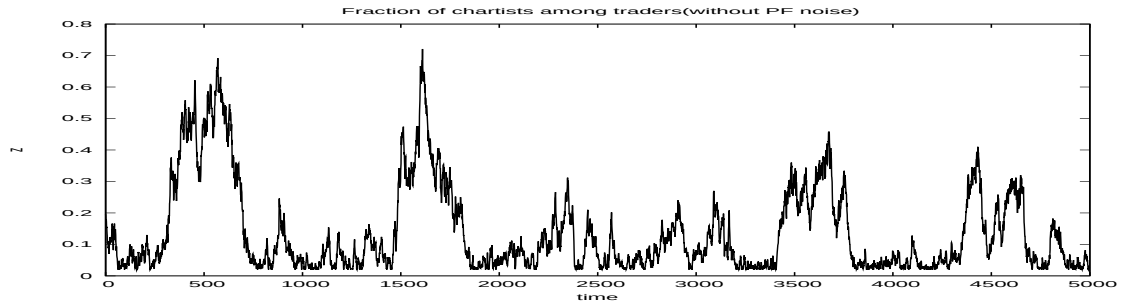

(c)

Figure 4.24: Simulation results of the Lux-Marchesi model when μ is adopted as the only source of noise. (a) Price evolution. (b) Time series of log-return. (c) Evolution of the fraction of chartists.

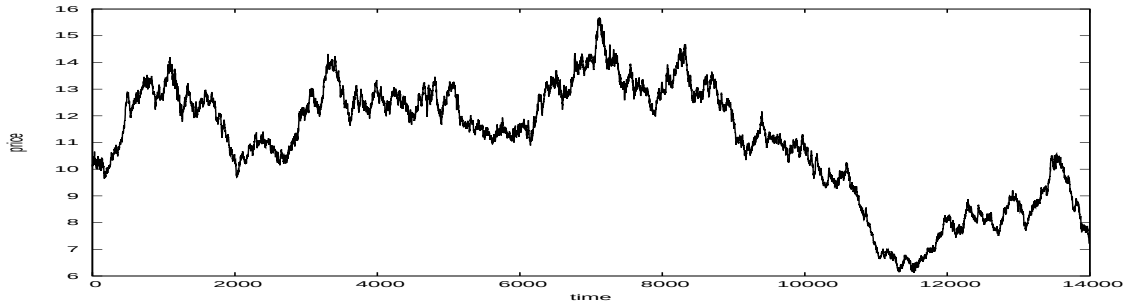

(a)

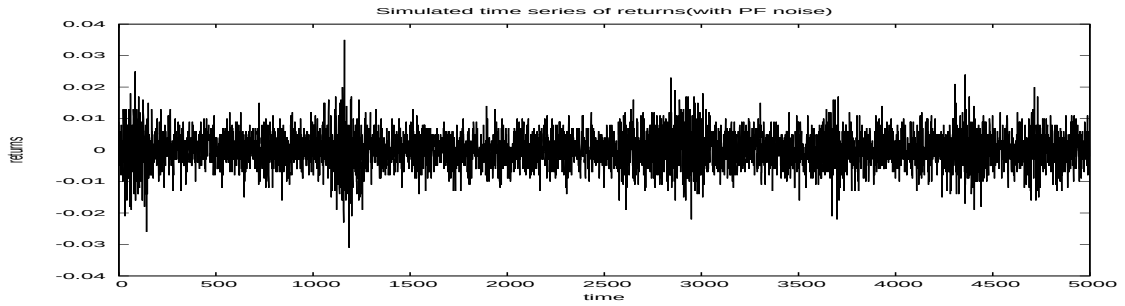

(b)

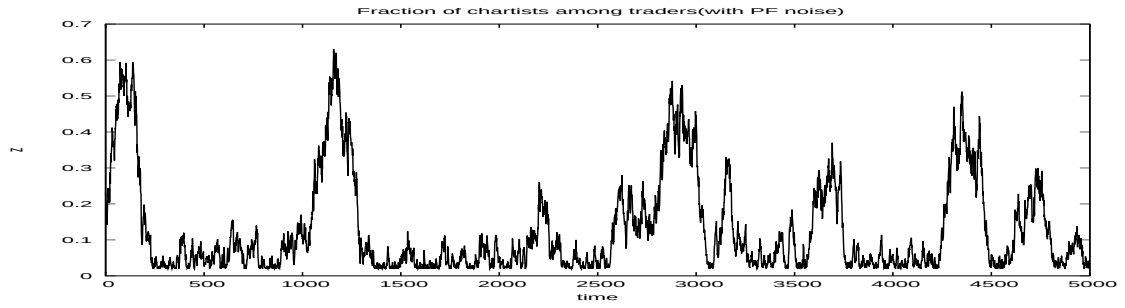

(c)

Figure 4.25: Simulation results of the Lux-Marchesi model when we only take the uncertainty in the fundamental value. (a) Price evolution. (b) Time series of log-return. (c) Evolution of the fraction of chartists.

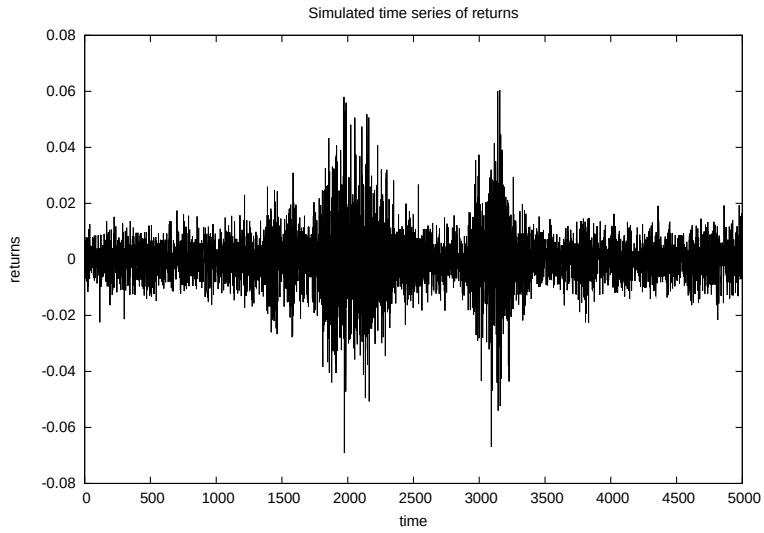

(a)

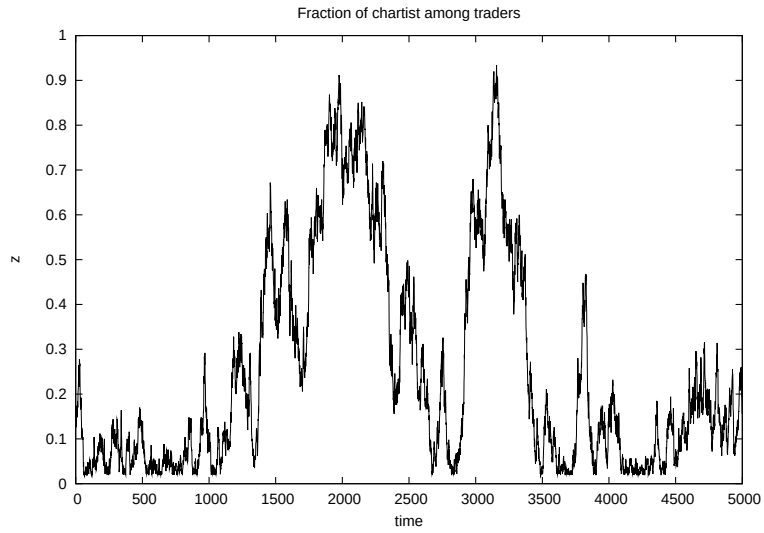

(b)

Figure 4.26: (a) simulated time series of log price returns, with fundamental price and excess demand noise of μ . (b). simulated time series of fraction of chartists. $z = n_c/N$. With noise of fundamental price and noise of μ in price adjustment.

Probability distribution of returns

Figure 4.27 presents the PDF of return for the three situations with regard to varying level of noise. Figure 4.27(a), 4.27(b) and 4.27(c) are, respectively, the PDFs corresponding to the case when only the noise term μ is used, only the noise in the fundamental value is adopted, and both noises are chosen.

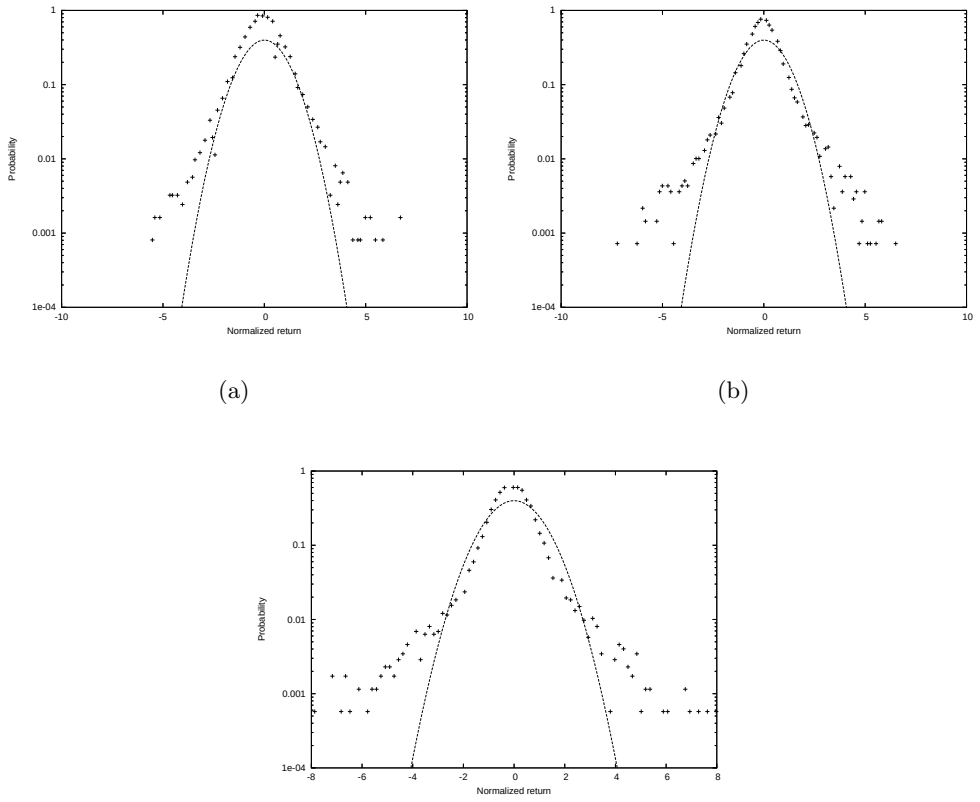

(a) (b)

(c)

Figure 4.27: (a) PDF of return of the case that μ is the only noise. (b) PDF of return of the case that only the source of uncertainty in the fundamental price is adopted. (c) PDF when both types of noise are included.

We further study the properties of the probability density function of return at different levels of time aggregation, *i.e.* the values of τ in $ln(p_{f,t}) = ln(p_{f,t-\tau}) + \epsilon_t \Delta t$. The corresponding PDFs are shown in Figure 4.28. This plot demonstrates that less value of τ leads to fatter tails; increasing the value of τ give rise to PDFs close to the Gaussian distribution. This confirms the observation on empirical data discussed in Chapter 2 that lower frequency (larger τ) financial data exhibits more features close to Gaussian distribution.

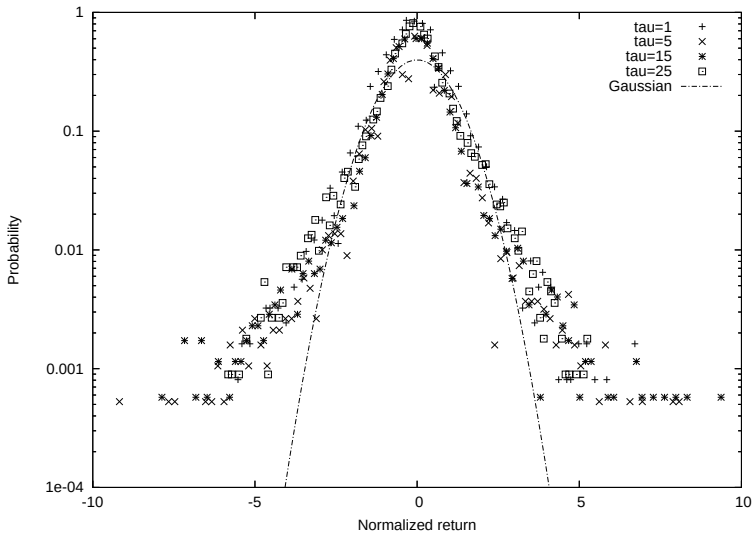

Figure 4.28: PDFs at different level of time aggregation.

Autocorrelation of returns

To measure the effect of volatility clustering, we calculate and plot the autocorrelations of the simulated return, squared return and absolute return. All the situations discussed above are investigated. Figure 4.29 shows the corresponding ACF plots for the case with fundamental noise and the case without fundamental price noise, respectively.

Both plots show that autocorrelations of return fluctuate around zero, indicating lack of memory in return. However, squared and absolute returns (volatility) possess autocorrelations for long time. In addition, when the noise of fundamental price is present, the autocorrelations of squared and absolute returns decay more slowly that the other case.

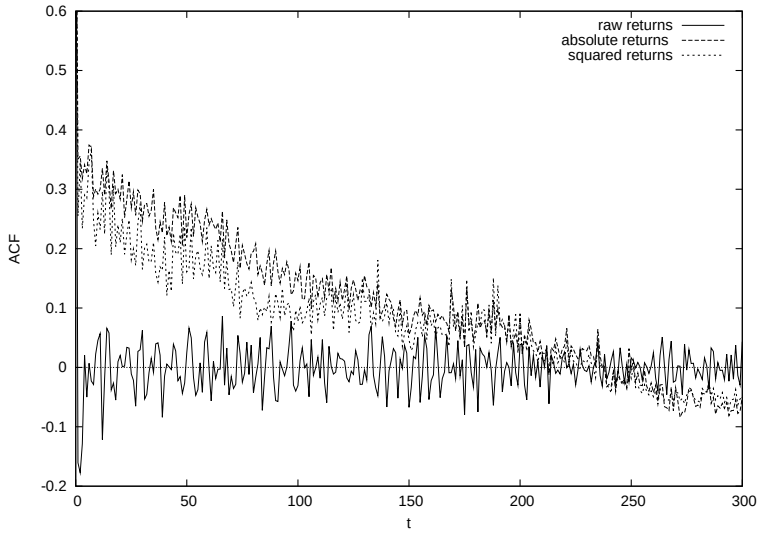

(a)

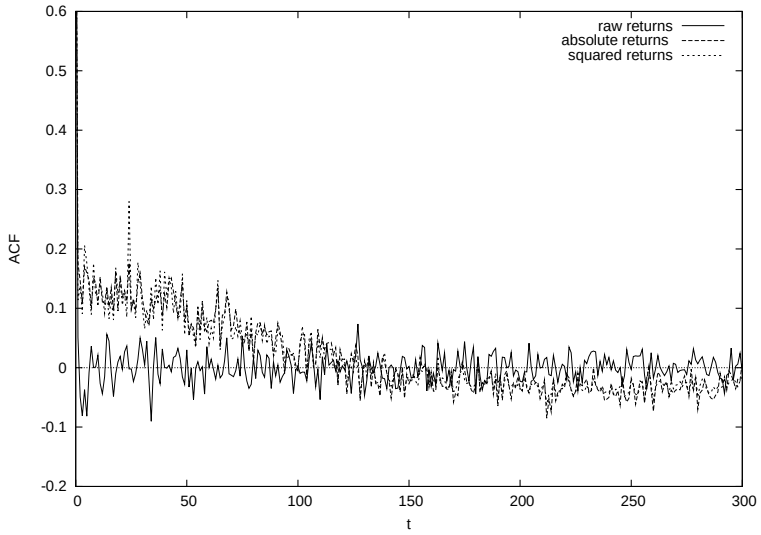

(b)

Figure 4.29: (a) The ACF of return (the lowest one), squared return (the middle one) and absolute return. Fundamental price is fixed to 10. (b) The ACF of return (the lowest one), squared return (the middle one) and absolute return. Changes of fundamental price follow a Gaussian distribution with mean 0 and deviation 0.0005.

4.3.3 Discussion

This model is suitable for simulating low frequency market dynamics, considering that traders need time to compare the performances of different strategies and make decision to switch among them. The movement of the traders among the different groups is the key of the dynamics. The periods of high fractions of chartists correspond to the periods of large clusters of high return.

The Lux-Marchesi model reproduces most of the main stylized facts including the "fat tails" distribution of return, and volatility clustering. However, this model does not apply to a market with large number of traders. We have carried out a series of experiments concerning the influence of number of agents. In the experiments the number of agents were varying from 500 to 100000. Figure 4.30 shows the simulation results of z when the number of agents is set to 500, 5000, 50000 and 100000, respectively. For each experiment, the fraction of chartist among all agents is initially set to 20%. For small N, for example 500 or 5000, the returns show strong fluctuations and clustering of volatility. As N becomes larger, it shows that z quickly falls to zero with little fluctuations. Consequently, the returns exhibit much weaker or no volatility clustering, the price is closer to the fundamental price. Thus, large number of agents may significantly change the dynamics generated by the Lux-Marchesi model. These results are consisted with that of [10].

Another drawback of the Lux-Marchesi model is that the simulation time required is much longer than that required by the other two models. Our simulation program was implemented in JAVA. One simulation took about several hours on a machine with 2.80 GHZ Pentium 4 and 512 MB memory, when using 1000 traders. One of the reasons for this is that the Lux-Marchesi model has more types of trader (three) than the Bak model (two) and the Cont-Bouchaud model (one). Moreover the rules are more complicated than those of the other two models. Another important reason is that at every time step, *every* agent needs to compare his profitability with other agents and a new probability of switching needs to be determined, while in the Bak model in every time step, there are only two agents in the transaction, and only those two agents' behavior are considered. Moreover, in the Cont-Bouchaud model, the random graph structure is formed only once in the beginning, the price calculation is calculated at a group level whose sizes are not changed through the simulation.

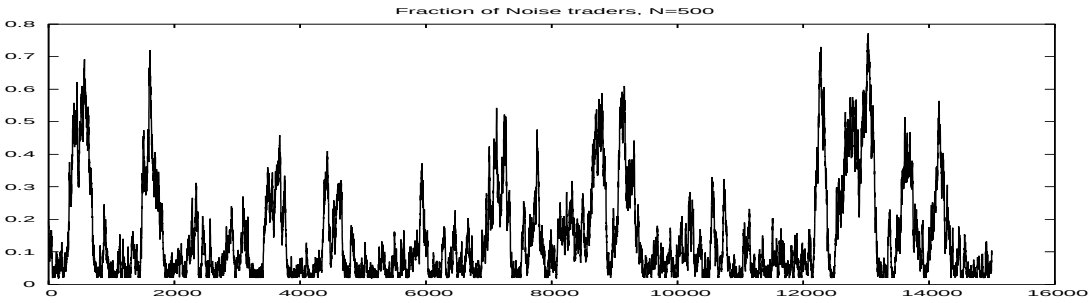

(a)

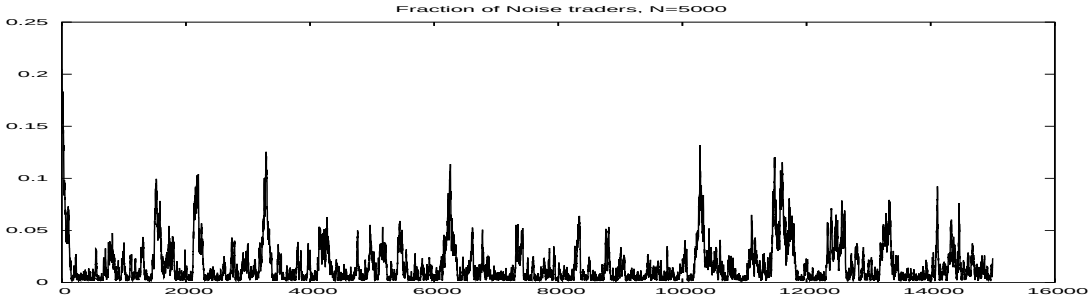

(b)

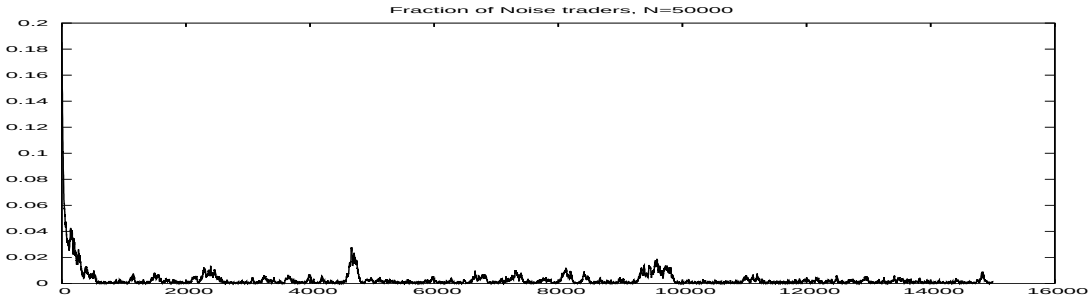

(c)

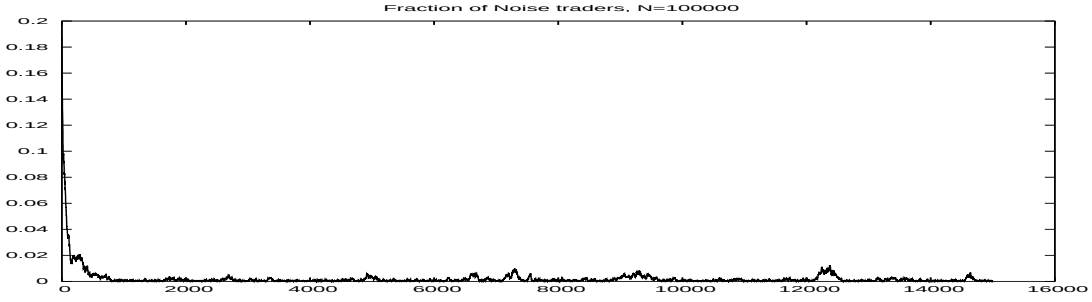

(d)

Figure 4.30: Evolution of fraction of chartists of different cases in terms of total number of traders. (a). $N = 500$, (b). $N = 5000$, (c). $N = 50000$ and (d). $N = 100000$. The scale of vertical axes in the various plots are :(a) $0 - 0.8$, (b) $0 - 0.2$, (c)$0 - 0.06$ and (d) $0 - 0.04$. The scale of the horizontal axis is $0 - 150000$.

Chapter 5

Improvements of the Cont-Bouchaud Model

5.1 A Critical Problem of the Cont-Bouchaud Model

In the last chapter, we stated that although the Cont-Bouchaud model can successfully generate non-Gaussian (fat-tailed) distribution of return, it cannot confirm another important stylized fact: volatility clustering. Indeed, the relation between 'fat tails' and volatility clustering is not straightforward. According to our experiments, data that exhibit volatility clustering always have a 'fat-tailed' distribution, but the opposite is not always true. A set of data presenting fat tails in its PDF plot may contain many relatively large values, but these values could be evenly distributed over time rather than clustered together. This effect can be observed in the time series (of return) that are generated by the Cont-Bouchaud model. Since volatility clustering is ubiquitous in financial time series, the inability to confirm volatility clustering is a critical problem of the Cont-Bouchaud model.

As pointed out in chapter 4, this problem is a direct consequence of the behavior of the agents in the Cont-Bouchaud model. This model assumes that at each time step, if the agents are going to trade, their demands (either $+1$ or -1) are randomly determined. There is no direct or indirect dependence between the demands at successive time steps. We have put some effort in improving this model by introducing relations among the agents behavior at successive time steps. In the rest of this thesis, we will present our improvements and results.

5.2 Our solutions

Knowledge about the *origin* of volatility clustering in real markets is undoubtedly helpful if we want to improve the Cont-Bouchaud model. Unfortunately, there is not yet a widely accepted explanation for this phenomenon in the finance community. In his recent paper [13], Cont listed four possible mechanisms:

- Heterogeneous arrival rates of information;
- Co-existence and evolution of strategies;
- Behavioral switching;
- Investor inertia.

However, we believe that, no matter which mechanism accounts for the origin, it influences volatility through its impact on the *activity* of agents. This argument is based on the observation that there is a positive correlation between trading volume and volatility [8]. Here, we argue that there is a strong correlation between trading volume and activity: The more actively the agents participate in trading, the larger on average, their trading quantities are. The work of some researchers, as in e.g. [23], also support this argument.

The Cont-Bouchaud model does include the volume/volatility correlation to some extent, as *activity* ultimately is connected with the number of clusters that are participating in trading at a certain time step. Figure 5.1 shows the numerical results for price change when different values for the activity parameter are used. It shows the following: the higher the activity, the larger the (positive or negative) change in price in any period of time.

Based on these results, we feel that volatility clustering can arise from volume/volatility correlation, provided that activity changes over time. However, the original Cont-Bouchaud model lacks a mechanism through which activity can be directly or indirectly adjusted. Therefore we propose to add a mechanism of such kind in this model.

Some studies suggest a positive correlation between activity and price. For example, H.S Shin et al [5], investigated interactions between trading activities and prices in the US treasury market. Their studies confirm this relation. We introduce two alternative mechanisms of activity adjustment into the Cont-Bouchaud model. They are expressed in Equations 5.1 and 5.2.

1. Mechanism I

$$a(t) = min(a_0 + k_1 * \mid P - P_f \mid^b, 0.5). \tag{5.1}$$

   where P denotes the current price, $a_0 = 0.02$ the lower bound for the activity parameter, k_1 a constant, and b a parameter. P_f can be understood as an objective fundamental price. Basically, we link the activity to the deviation of the price from a benchmark. Here, we take the fundamental price as the benchmark. It should be noted that in this model we allow only one type of traders. Besides that, the exponent b indicates the sensitivity of the activity to price deviation. In our numerical experiments we will consider different values for b.

2. Mechanism II

$$a(t) = min(0.5, max(0, a_0 + k_2 * \frac{\sum \Delta P}{K}))) \tag{5.2}$$

where $\sum \Delta P$ denotes the sum of the price changes during the last K time steps, $a_0 = 0.02$ is the initial level of activity, and k_2 is a constant.

Instead of looking at the relation between activity and price level, we link activity to historical price changes. In this way, we include 'memory' into the dynamics. In this scheme, we take the average price change of the last K time steps to reflect the historical price changes.

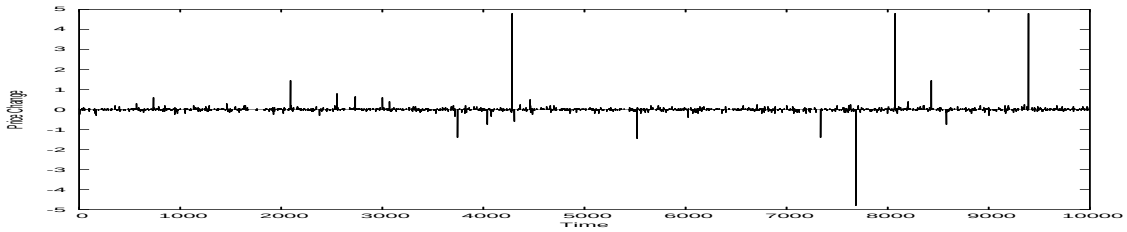

(a) a=0.0001.

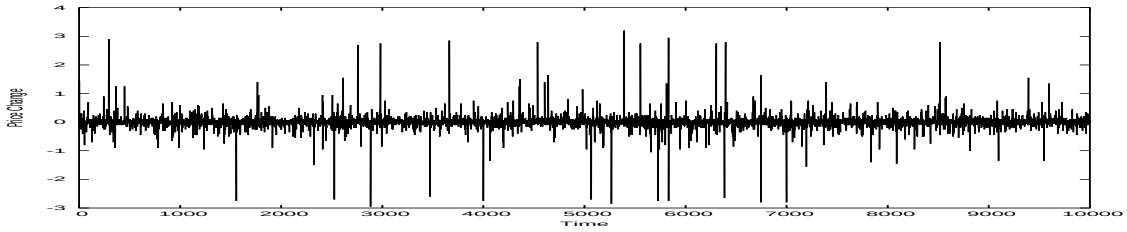

(b) a=0.001.

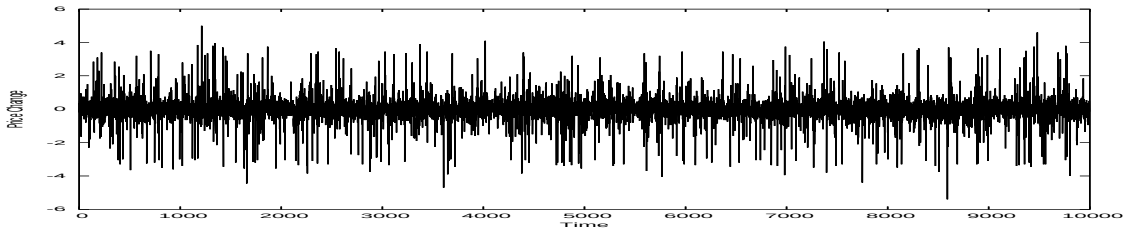

(c) a=0.01.

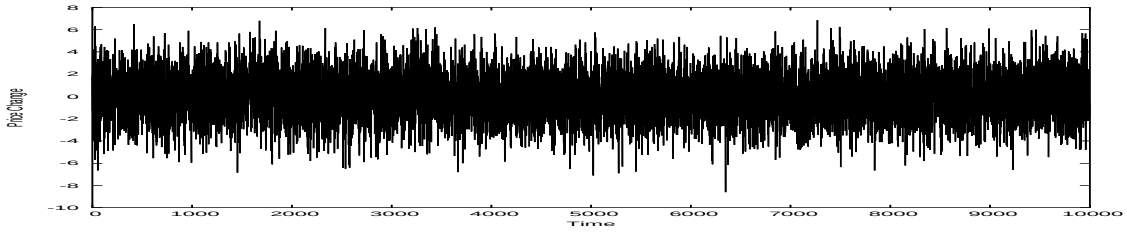

(d) a=0.2.

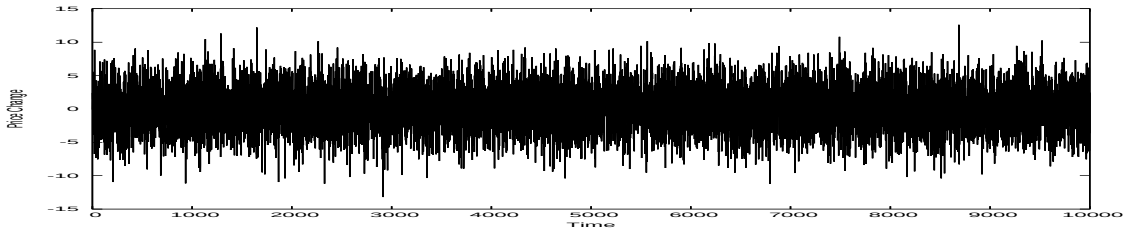

(e) a=0.45.

Figure 5.1: Price changes generated by the Cont-Bouchaud model when different values of activity are used in the simulations. Here, $N = 1000$ and $c = 0.9$. Note that the y axes of the plots are on different scales.

5.3 Simulation Results

1. The results of mechanism I

   Figure 5.2 shows the results that were obtained with Mechanism I. In this figure, the price change against activity, corresponding to different values of b are shown. We see that activity evolutions present continuous up and down movements. This adjustment of activity leads to volatility clustering. The latter is clearly illustrated in the results of all the cases.

   In addition, we show the autocorrelation of return and the autocorrelation of volatility for different different values of b (see Figure 5.3). They are in line with empirical observations, *i.e.* while time series of return lacks 'memory', data of volatility exhibit long-term temporal correlation.

2. The results of mechanism II

   Figure 5.4 presents the simulation results of price change and activity with Mechanism II. Volatility clustering is again clearly illustrated. Figure 5.5 further confirms these volatility clustering by drawing the autocorrelation function plot of their raw and absolute return.

5.4 Discussion

To explore the possibility possibility of introducing volatility clustering in Cont-Bouchaud model, we started with analyzing the relation between activity and volatility clustering. It was realized that activity adjustment may lead to this stylized feature. Then, based on the results of some empirical studies about the relation between activities and prices, we introduced two mechanisms into the model, which link activity to price level or historical price changes.

In our improved Cont-Bouchaud model, the *activity* of the agents, indicating how strongly they participate in trading, is regulated by the price level or historical price changes. These are what we have added upon the original model. Results obtained with this Cont-Bouchaud model show clearly volatility clustering.

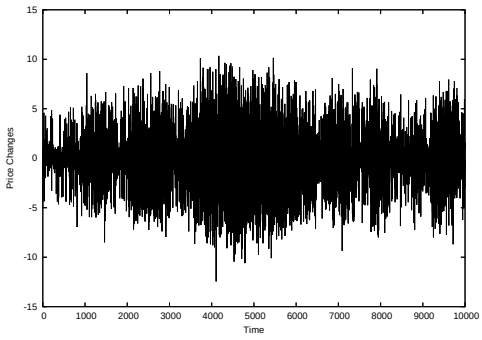

(a) Time evolution of price change when $b = 0.5$.

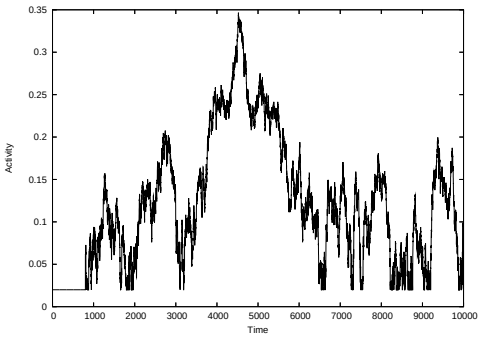

(b) Time evolution of activity when $b = 0.5$.

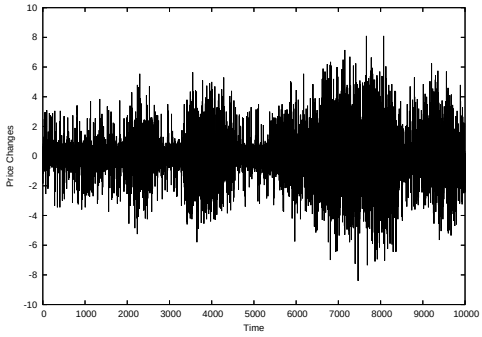

(c) Time evolution of price change when $b = 1.0$.

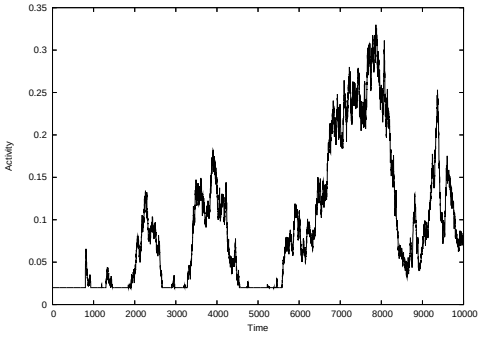

(d) Time evolution of activity when $b = 1.0$.

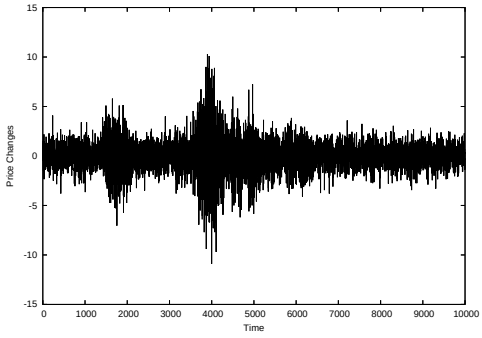

(e) Time evolution of price change when $b = 2.0$.

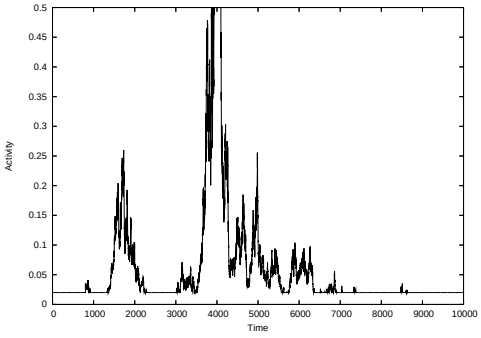

(f) Time evolution of activity when $b = 2.0$.

Figure 5.2: Results of simulations with mechanism 1: Evolution of price change and activity for different values of b: In (a) and (b) $b = 0.5$; in (c) and (d) $b = 1.0$; in (e) and (f) $b = 2.0$. Volatility clustering is produced in all these cases. Here: $N = 1000$ and $c = 0.9$.

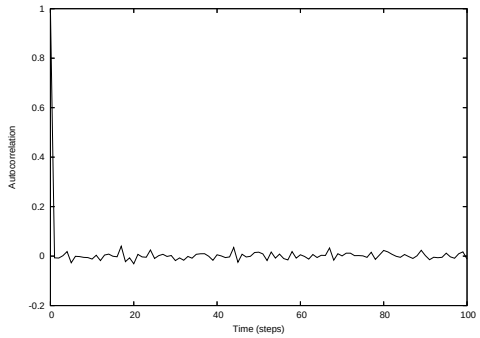

(a) ACF of raw return when $b = 0.5$.

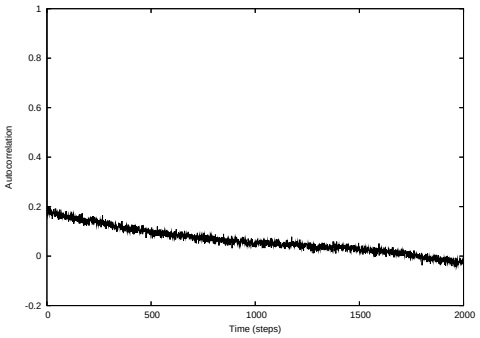

(b) ACF of absolute return when $b = 0.5$.

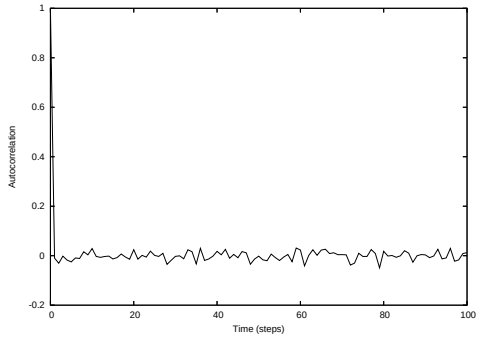

(c) ACF of raw return when $b = 1.0$.

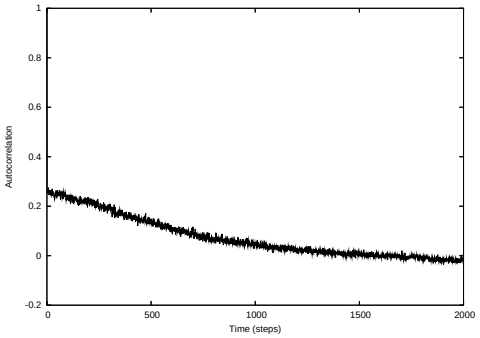

(d) ACF of absolute return when $b = 1.0$.

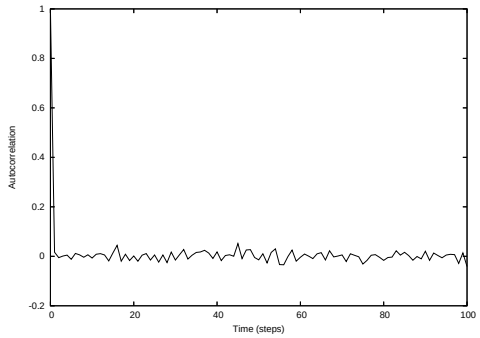

(e) ACF of raw return when $b = 2.0$.

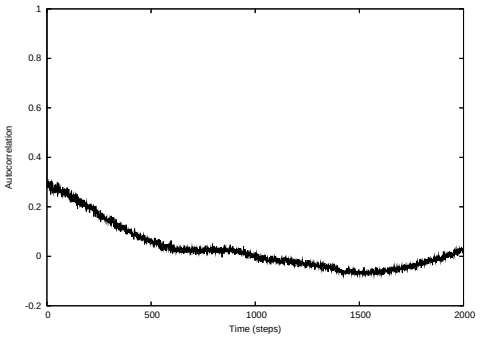

(f) ACF of absolute return when $b = 2.0$.

Figure 5.3: Results of simulations with mechanism I: ACF of return and absolute return for different values of b: In (a) and (b) $b = 0.5$; in (c) and (d) $b = 1.0$; in (e) and (f) $b = 2.0$. Volatility clustering is produced in all cases. Here: $N = 1000$ and $c = 0.9$.

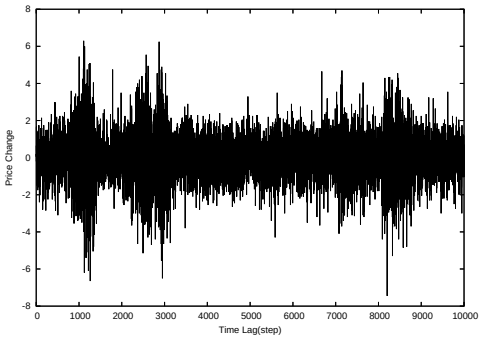

(a) K=10.

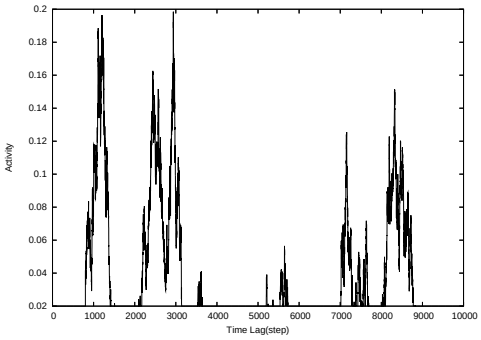

(b) K=10.

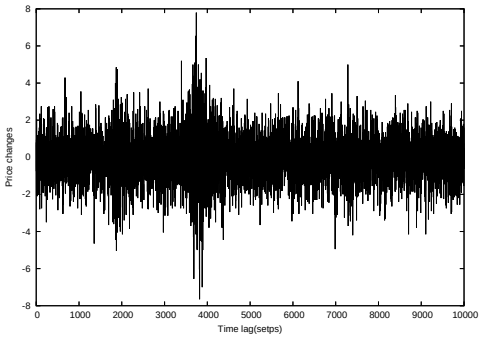

(c) K=20.

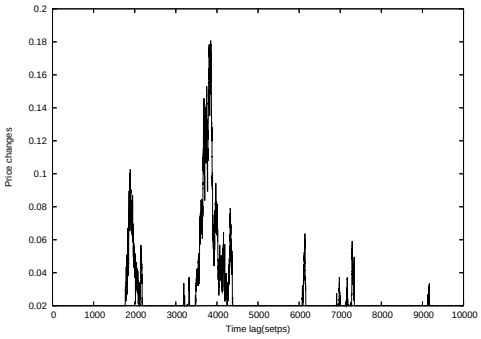

(d) K=20.

Figure 5.4: Results of simulation with Mechanism II: Evolution of price change and activity for different values of K: In (a) and (b) $K = 10$; in (c) and (d) $K = 20$. In all figures $k_2 = 1$ is used.

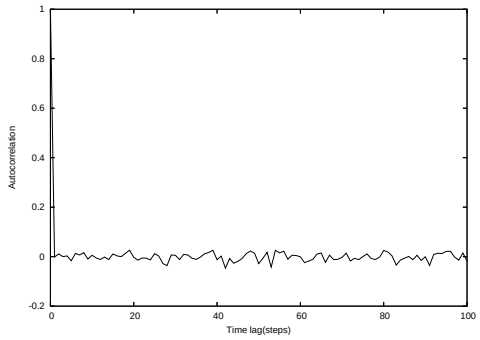

(a) ACF of raw return when K=10.

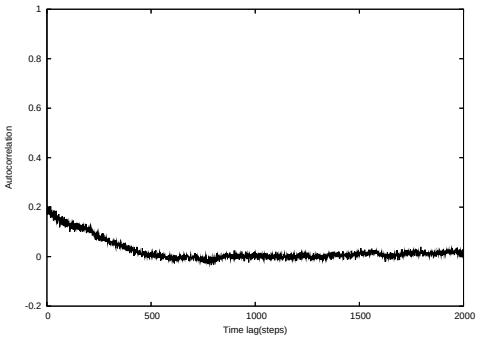

(b) ACF of absolute return when K=10.

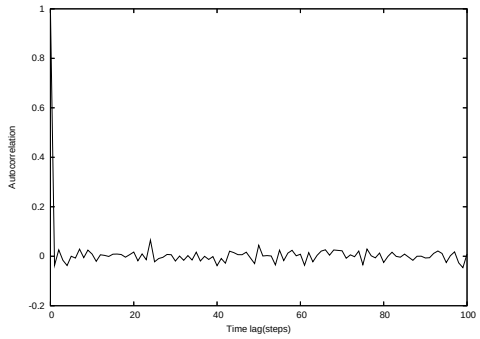

(c) ACF of raw return when K=20.

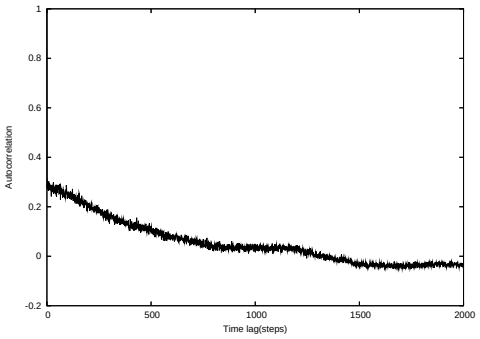

(d) ACF of absolute return when K=20.

Figure 5.5: Results of simulation with Mechanism II: ACF of raw and absolute return for different values of K: In (a) and (b) $K = 10$; In (c) and (d) $K = 20$. In all figures $k_2 = 1$ is used .

Chapter 6

Conclusions and Future work

6.1 Conclusions

6.1.1 Confirmation of the Stylized Facts by Microsimulation Models

The complex dynamics of financial markets can be characterized by some stylized facts. Among these, the fat-tailed distribution of return and volatility clustering are the most mysterious and they have been widely discussed. Microsimulation, a complementary approach for modeling and simulation in economics and finance, has been used by more and more researchers to understand this complex dynamics. Among the many microsimulation models developed in the recent years, we have chosen three well-known models to explore in detail in this research. We have performed thorough investigations of these models for a wide range of parameter settings. Table 6.1 provides a summary of these models in terms of the modeling scheme and their capability to confirm the stylized facts.

All three models can produce fat-tailed distribution of return (or price change). The common trait of these model that accounts for the non-Gaussian distribution is the *herding* behavior. The Cont-Bouchaud model describes herding as the process of the formation of groups of agents and the harmonization

Table 6.1: Summary of three well-known microsimulation models.

	C-B model	Bak model	Lux model
Agent classification	homo-geneous	hetero-geneous	hetero-geneous
Characteristic agent behavior	group formation	price diffusing, copying and drifting	strategy switching
Confirmation of fat-tailed distribution of return	yes	yes	yes
Confirmation of volatility clustering	no	yes	yes

of the action of the agents belonging to same group. The Bak model models it as follows: The trading agent randomly picks another agent in the market and copies his price or the agent drifts his price towards the market price, which of course was the trading price of another agent in a previous time step. According to the Lux model, herding is the tendency of agents to switch their strategies to the one being taken by the agent who has made more profits.

Among the three, the Bak model and Lux model can generate volatility clustering, while the Cont-Bouchaud model cannot. According to the Bak model, the cause of volatility clustering is related to *volatility feedback*: The strength of the drift in price is proportional to the actual recent variations in market price. The analysis of the simulation results obtained from the Lux model reveals a different cause. According to this model, during different time periods, the fraction of chartists (fundamentalists) changes over time. Higher fractions of chartists correspond to higher average trading activities.

The inability of the Cont-Bouchaud model to confirm volatility clustering is due to the methodology that is used to determine the demand of the different clusters. According to this model, at each time step, the demand of a group of agents is randomly determined, i.e. they are not dependent on the demand at previous time steps.

6.1.2 Our Modifications and Contributions

We have benefited from the implementation of the three well-known models to further understand the complex dynamics of financial markets. In particular, we have identified the common grounds of these models with respect to the explanation of the most important stylized facts: non-Gaussian (fat-tailed) distributions of return and volatility clustering. Namely, the reason of the former is mainly associated with herding behavior; that of the latter is related to the time evolution of the activity level. Numerical experiments with these models show that the fat-tailed distribution of return does not imply volatility clustering. The component that is indispensable for the generation of volatility clustering, although explained differently by these models, is a factor that links volatility level to the activity of agents.

It is this point that guided our work in improving the Cont-Bouchaud model. We have introduced two mechanisms into the model to relate the activity parameter to the level of price change. Our improved model robustly produces the volatility clustering phenomenon.

6.2 Directions for Future Work

Based on the results of our current work, we propose some interesting directions for future research on this topic.

6.2.1 Development of a generic environment

A generic environment for microsimulation of financial markets will be very helpful for future research on this topic. This environment may consists of

different layers: A core layer that contains different rules with respect to the behavior of the agents; an application layer that gathers the input data such as the description of all agents, the number of agents, stock assets etc.; and an output layer that generate data sets in a standard format, or further generates the plots using some integrated tools.

6.2.2 Application of grid computing

When we increase the number of agents or divide the agents into more different groups with a different characterization, the workload of a typical simulation quickly reaches the computational limitations of our desktop computers. Grid computing can be considered as a promising technology for these computationally intensive simulations. Especially due to the fact that a large parameter space should be typically explored in which the individual simulations can be executed independently.

6.2.3 Quantitative analysis

So far, we have mainly dealt with qualitative analysis of the dynamics of the financial markets, although we have taken some numerical criteria such as kurtosis and autocorrelation to judge the character of the dynamics. A more rigorous quantitative characterization of the simulation results and a comparison with empirical data would be definitely interesting. Specifically, one can perform detailed analysis of the multi-fractal properties of empirical and simulated financial data [20].

Bibliography

[1] http://www.fool.com/school/indices/sp500.htm.

[2] http://www.investorwords.com/5803/statistical_arbitrage.html.

[3] http://mathworld.wolfram.com/SmallWorldNetwork.html.

[4] L Bachelier. Lthéorie de la spculation. *Annales Scientifiques de l'cole Normale Suprieure Sr*, 3(17), 1900.

[5] Benjamin H Cohen and Hyun Song Shin. Positive feedback trading in the us treasury market. *BIS Quarterly Review*, (June), 2002.

[6] R. Cont and J-P. Bouchaud. Herd behavior and aggregate fluctuations in financial markets. *Macroeconomic Dynamics*, 4(170-196), 1997.

[7] R Cont, JP Bouchaud, and M Potters. *Scaling in financial data: stable laws and beyond*. Springer, Berlin, 1997.

[8] Rama Cont. Empirical properties of asset returns: stylized facts and statistical issues. *Quantitative Finance*, 1(2):223–236, 2001.

[9] Rama Cont and Peter Tankov. *Finaicail Modelling With Jump Process*. Chapman & Hall/CRC Press, UK, 2004.

[10] E Egenter, T Lux, and D Stauffer. Finite-size effects in monte carlo simulations of two stock market models. *Physica A*, 268, 1999.

[11] Fama E F. Efficient capital markets ii. *Journal of Finance*, (461):575–613, 1991.

[12] John C. Hull. *Option, Futures & Other Derivatives*. Cambridge University Press, The Edinburgh Building, Cambridge, CB2 2RU, UK, 2000.

[13] Giardina I. and Bouchaud J.-P. *Volatility clustering in agent based market models*, volume 324. Springer, Berlin, 2003.

[14] Haim Levy, Moshe Levy, and Sorin Solomon. *Microscopic simulation of financial markets*. Prince Hall Press, Prince Hall, New Jersey 07458, US, fifth edition edition, 2003.

[15] Thomas Lux. Herd behavior, bubbles and crashes. *The Economic Journal*, 105, 1995.

[16] Thomas Lux. The stable paretian hypothesis and the frequency of large returns: An examination of major german stocks. *Applied Financial Economics*, 6, 1996.

[17] Thomas Lux. The socio-economic dynamics of speculative markets: interacting agents, chaos, and the fat tails of return distributions. *Journal of Economic Behavior & Organization*, 33, 1998.

[18] Thomas Lux and Michele Marchesi. Scaling and criticality in a stochastic multi-agent model of a financial market. *Nature 397*, 20(498), 1999.

[19] B Mandelbrot. The variation of certain speculative prices. *The Journal of Business*, 36(4):392–417, 1963.

[20] R. N. Mantegna and H. E. Stanley. *An Introduction to Econophysics*. Cambridge University Press, Cambridge, UK, 2000.

[21] J. Menke, H. S. Hassan, N. Sluijs, and Z. Rahhal. Mirco simulation of financial markets:. Technical report, Universiteit van Amsterdam, 2005.

[22] P.Bak, Paczuski, and M.Shubik. Price variations in a stock market with many agents. *Physica A*, 246, 1997.

[23] P.Gopikrishnan, V.Plerou, and H. E. Stanley. Price fluctuations and market activity. *Physica A*, (229), 2001.

[24] G. Qiu, D. Kandhai, and P.M.A. Sloot. Understanding the complex dynamics of financial markets through cellular automata. To be submitted.

[25] F van der Ploeg. *The handbook of international macroeconomics*. Oxford University Press, Oxford, UK, 1994.

[26] Johannes Voit. *The Statistical Mec hanics of Financial Markets*. Springer, Berlin, 2003.

[27] Wikipedia. http://www.wikipedia.org/wiki/Stock_market_index.html.

[28] W. Willinger, M.S. Taqqu, and V. Teverovsky. Long range dependence and stock returns. *Finance and Stochastics*, (3):1–13, 1999.